Structural Engineering

EVALUATION OF NBCC FUNDAMENTAL PERIOD FORMULAE USING AMBIENT VIBRATION DATA – LITERATURE REVIEW OF RELEVANT TOPICS

By Damien Gilles

Approved by Prof. Ghyslaine McClure

11 August 2008

Structural Engineering Series Report No. 2008-02

Department of Civil Engineering
and Applied Mechanics

McGill University
Montreal

Evaluation of NBCC Fundamental Period Formulae Using Ambient Vibration Data

Literature review of relevant topics

By

Damien Gilles

August 2008

Department of Civil Engineering and Applied Mechanics

McGill University

Structural Engineering Series No. 2008-02

Foreword

The author and his supervisor, Prof. Ghyslaine McClure, are currently undertaking a research project aimed at evaluating the fundamental period formulae in the 2005 edition of the National Building Code of Canada (NBCC) using ambient vibration data. This report is a review of relevant literature and methods. The topics covered include fundamental structural dynamics concepts, seismic design provisions in Canada, a review of empirical formulae used to calculate the fundamental periods of structures, experimental modal analysis, ambient vibration testing, stochastic processes and signal processing techniques.

Table of Contents

List of Figures

List of symbols

SDOF Oscillators

c	Viscous damping coefficient
$f(t)$	Instantaneous excitation
$h(t)$	Impulse response function (IRF)
k	Stiffness
m	Mass
S_d	Displacement response spectrum
S_v	Pseudo-velocity response spectrum
S_a	Pseudo-acceleration response spectrum
t	Time variable
t_m	Time at which maximum displacement occurs
$u(t)$	Instantaneous relative displacement
$\dot{u}(t)$	Instantaneous relative velocity
$\ddot{u}(t)$	Instantaneous absolute acceleration
$\ddot{u}_g(t)$	Instantaneous ground acceleration
u_{max}	Maximum relative displacement
V_{max}	Maximum base shear
W	Weight
ξ	Viscous damping ratio
ω_n	Undamped natural circular frequency (rad/s)
ω_d	Damped natural circular frequency (rad/s)

MDOF Oscillators

$[C]$	Viscous damping matrix
$\{F(t)\}$	Excitation vector
$[K]$	Stiffness matrix
K_r	Modal stiffness corresponding to mode *r*
$[M]$	Mass matrix
M_r	Modal mass corresponding to mode *r*
$\{q(t)\}$	Vector of modal coordinates

$q_r(t)$	Modal coordinate corresponding to mode *r*
$\{u(t)\}$	Relative displacement vector
$\{\dot{u}(t)\}$	Relative velocity vector
$\{\ddot{u}(t)\}$	Absolute acceleration vector
$\lvert u_r \rvert_{\max}$	Maximum modal displacement corresponding to mode *r*
$\lvert u \rvert_{\max}$	Maximum displacement (SRSS combination)
$[\Phi]$	Mode shape matrix
$\{\phi_r\}$	Mode shape vector for mode *r*
ω_r	Natural frequency corresponding to mode *r* (rad/s)
ξ_r	Modal damping ratio for mode *r*
λ_r	Complex pole for mode *r*

Fourier Analysis

a_n	Real coefficient of the cosine part of a real Fourier series
b_n	Real coefficient of the sine part of a real Fourier series
$F(\omega)$	Frequency domain representation of the excitation
$\{F(\omega)\}$	Vector of Fourier coefficients of the excitation
$F_k(\omega)$	Frequency domain representation of the excitation at DOF *k*
$H(\omega)$	Frequency response function (FRF)
$H_{jk}(\omega)$	FRF between output *j* and input *k*
$[H(\omega)]$	Matrix of FRFs
$i = \sqrt{-1}$	Basic imaginary number
T_1	Period of a periodic function (Fourier series)
$U(\omega)$	Frequency domain representation of the displacement
$\{U(\omega)\}$	Vector of Fourier coefficients of the response
$U_j(\omega)$	Frequency domain representation of the displacement at DOF *j*
$x(t)$	General time history function
$X(n)$	Complex Fourier coefficient of a harmonic of frequency $n\Omega_1$ (Fourier series)
$X(\omega)$	Complex Fourier coefficient at frequency ω

$\left[P_{ff}(\omega)\right]$	Auto-spectral density matrix of the input forces
$\left[P_{uu}(\omega)\right]$	Auto-spectral density matrix of the output responses
ϕ_{jr}	Element of mode *r* corresponding to DOF *j*
ω	Circular frequency variable (rad/s)
Ω_1	Frequency of a periodic function (Fourier series)

Fundamental Period Studies

D_f	Length of the building or of the lateral load resisting system, parallel to the applied seismic forces (in feet)
h_f	Height of the building above ground (in feet)
h_m	Height of the building above ground (in metres)
N	Number of storeys
T	Fundamental period (in seconds)

Experimental Modal Analysis

$H_1(\omega)$	FRF estimator
$H_2(\omega)$	FRF estimator
$H_3(\omega)$	FRF estimator
$P_{ff}(\omega)$	Auto-spectral density of the input (*f*)
$P_{fu}(\omega)$	Cross-spectral density between input (*f*) and output (*u*)
$P_{uf}(\omega)$	Cross-spectral density between output (*u*) and input (*f*)
$P_{uu}(\omega)$	Auto-spectral density of the output (*u*)
$\gamma^2(\omega)$	Ordinary coherence function for FRF estimates

Random Processes

$P_{xy}(\omega)$	Cross-spectral density between random signals *x(t)* and *y(t)*
$R_{xx}(\tau)$	Autocorrelation function of process *x(t)*
$X^m(\omega)$	Fourier spectrum of *x(t)* calculated from window *m*
$Y^m(\omega)$	Fourier spectrum of *y(t)* calculated from window *m*
μ_x	Mean of process *x(t)*

Data Treatment

f_b	Frequency included in SDOF bell function

f_p	Resonance frequency identified from peak in singular value plot
N	Number of DOFs where ambient records were collected
$[P]$	Spectral density matrix
$P_{jk}^m(\omega)$	Cross-spectral density between $x_j(t)$ and $x_k(t)$ for window m
$P_{jk}(\omega)$	Averaged spectral density between $x_j(t)$ and $x_k(t)$
$[S]$	Diagonal singular value matrix
s_j	j^{th} Singular value
$[U]$	Matrix of left-singular vectors
$\{u_j\}$	j^{th} Singular vector
$[V]$	Matrix of right-singular vectors
$x_i(t)$	Ambient record collected at DOF i
$x_i^m(t)$	Sub-record (window) of $x_i(t)$
$y_i^m(t)$	Modified sub-record
$Y_i^m(\omega)$	Fourier spectrum obtained from modified sub-record for DOF i
$\{\phi_p\}$	Normalized mode shape corresponding to resonance frequency f_p

Mathematical operators

$[\cdot]^H$	Hermitian transformation (complex conjugate transpose)
$E[\cdot]$	Expected value operator
*	Complex conjugate operator
$\left\| \cdots \right\|$	Absolute value of a real number or norm of a complex number
$\left\Vert \cdots \right\Vert$	Vector norm

Note: Symbols used in section 3 relating to the NBCC provisions are defined directly in the text since they have changed significantly over the years.

1. Introduction

It has long been recognized that earthquakes have the potential to cause significant damage and loss of life, a fact that continues to manifest itself around the world virtually every time an earthquake occurs. Since the early 1930s, significant efforts have been made to provide an adequate level of protection against earthquakes to engineered structures, by specifying rational seismic design guidelines. As the state of knowledge about the governing mechanisms responsible for seismic activity and the effects of seismic ground motions on structures has progressed, so too has the refinement of the seismic design provisions.

In Canada, a method for treating the seismically-induced forces was introduced in the very first edition of the National Building Code, in 1941. Periodic changes were made to these guidelines to reflect the evolution in knowledge. At the time of writing this, 12 editions of the National Building Code of Canada have been released. In this report, a critical review of the changes to the seismic design requirements for buildings in Canada, according to the National Building Code of Canada, will be presented and discussed.

Further, since the 1970 edition of the NBCC, the lateral seismic design forces for a structure are specifically estimated as a function of its fundamental lateral vibration period. However, this parameter cannot be determined accurately before a structure is built. Therefore, building codes typically specify simple empirical formulae based on global building geometry to estimate the fundamental period of structures. A critical review of these formulae will also be presented.

In evaluating the adequacy of these period formulae, it is essential to compare them with period data from actual buildings. Ideally, this information would be obtained during significant ground shaking events, since it is expected that the period will elongate as a function of the intensity of the ground motion (Udwadia and Trifunac 1974). However, this presents an important challenge, particularly in areas of low to moderate seismic activity, such as Eastern Canada and Montreal, since significant earthquakes occur only rarely. In such instances, the use of low amplitude ambient vibrations is a viable alternative. The topic of vibration testing to obtain the modal characteristics of full-scale structures will also be reviewed, with emphasis on ambient vibration testing.

Finally, certain issues relating to the treatment of ambient vibration data will be discussed. In particular, two common frequency domain modal parameter identification algorithms will be introduced.

2. Structural Dynamics Concepts

The response of structures to earthquake ground motion is a complex, dynamic phenomenon. Building codes aim to provide simple guidelines to account for these complex effects. Before discussing the history of seismic design provisions in Canada, it is important to understand a few key structural dynamics concepts, which form the very foundation of these guidelines. These concepts will also help understand the objectives and methods involved in experimental modal analysis (section 5). The following discussion is standard textbook material, summarized mainly from Craig and Kurdila (2006), and therefore few references will be used in the text for conciseness. Other excellent structural dynamics references include Chopra (2001), Clough and Penzien (2003), and Humar (2002).

2.1 Response of a linear SDOF system to general excitation

The equation of motion of a viscously damped linear elastic single-degree-of-freedom (SDOF) oscillator, subject to general dynamic excitation is

$$m\ddot{u}(t) + c\dot{u}(t) + ku(t) = f(t), \tag{2.1}$$

By considering the applied force, *f(t)*, as a series of impulses occurring at time τ, the response of the SDOF system can be obtained using the convolution (or Duhamel) integral

$$u(t) = \int_o^t f(\tau)\, h(t-\tau)\, d\tau, \tag{2.2}$$

where *h(t)* represents the unit impulse response function (IRF). For an SDOF oscillator having undamped natural frequency ω_n, damped natural frequency ω_d, and damping ratio ξ, the unit impulse response function is:

$$h(t) = \frac{1}{m\omega_d} e^{-\xi\omega_n t} \sin\omega_d t. \tag{2.3}$$

The other responses ($\ddot{u}(t)$, $\dot{u}(t)$, etc.) can be derived from the displacement function.

2.2 Frequency domain response of an SDOF system to general excitation

Alternatively, the solution can be obtained in the frequency domain by making use of the Fourier Transform of the input forces and the Frequency Response Function (FRF) of the system.

2.2.1 Fourier Series

Any continuous, periodic function can be represented by an infinite sum of discrete harmonics, each having its own frequency, amplitude and phase. Consider a continuous, general time history function, *x(t)*, having period T_1 and corresponding fundamental circular frequency, $\Omega_1 = 2\pi/T_1$. Then, it can be represented by an infinite series of discrete harmonics.

$$x(t) = \sum_{n=0}^{\infty} \left[a_n \cos(n\Omega_1 t) + b_n \sin(n\Omega_1 t) \right], \qquad [2.4]$$

In the above equation, a_n and b_n are scalar coefficients. Alternatively, a complex harmonic representation can be used.

$$x(t) = \sum_{n=-\infty}^{\infty} X(n) e^{i(n\Omega_1 t)}, \qquad [2.5]$$

where

$$e^{i\theta} = \cos\theta + i\sin\theta. \qquad [2.6]$$

As evident from this equation, *X(n)* represents the complex amplitude of a harmonic of frequency $n\Omega_1$. This is referred to as the Fourier coefficient, and is generally a complex quantity, calculated by the following integration, which is performed over a period.

$$X(n) = \frac{1}{T_1} \int_{\tau}^{\tau+T_1} x(t) e^{-i(n\Omega_1 t)} \, dt. \qquad [2.7]$$

2.2.2 Fourier Transform

Continuous, non-periodic functions require a slightly different treatment. By considering a non-periodic function to be a periodic function having a period which tends to infinity, a few modifications to the above equations lead to the well known Fourier integral transforms. Many forms of these equations appear in the literature. For the sake of consistency, the Fourier Transform pair using the circular frequency variable ω will be used here.

$$X(\omega) = \int_{-\infty}^{\infty} x(t) e^{-i(\omega t)} \, dt \qquad [2.8]$$

$$x(t) = \frac{1}{2\pi} \int_{-\infty}^{\infty} X(\omega) e^{i(\omega t)} \, d\omega \qquad [2.9]$$

The first equation is referred to as the (forward) Fourier Transform (FT) of *x(t)*, and the second, as the Inverse Fourier Transform (IFT) of *X(ω)*.

The Fourier Transform of *x(t)* will only exist if it satisfies the Dirichlet conditions (Proakis and Manolakis 1988):

1. *x(t)* has a finite number of discontinuities
2. *x(t)* has a finite number of extrema
3. *x(t)* is absolutely integrable, that is

$$\int_{-\infty}^{\infty} |x(t)|^2 \, dt < \infty \tag{2.10}$$

2.2.3 Discrete Fourier Transform

In practical applications, the function *x(t)* is sampled at constant time intervals for a finite amount of time, leading to a digital (non-continuous) representation of the function. Therefore, the Fourier integral transforms are not directly applicable, but rather a digital form known as the Discrete Fourier Transform must be used. Since the record length is finite, the Dirichlet conditions are almost always satisfied.

Consider a signal sampled at constant time intervals of Δt. A total of *N* sampled values are collected, representing a total sampling time of $T_1 = N \Delta t$. The total sample time is taken as one period of a periodic function. Therefore the continuous function *x(t)* is approximated by a periodic signal of period T_1, sampled at times $t_m = m\Delta t$, $m = 0,1,\ldots,(N-1)$. The frequency spacing of the Fourier Transform will be equal to the inverse of the record length $\Delta f = 1/T_1$ ($\Delta \omega = 2\pi/T_1$). The continuous time variable *t* is thus replaced by the discrete sampling times $t_m = m\Delta t$, and the frequency variable *ω* is replaced by discrete frequencies $n \Delta \omega$. This leads to the following expressions for the Discrete Fourier Transform (DFT) pair:

$$X(n \Delta \omega) = \sum_{m=0}^{N-1} x(t_m) e^{-i(mn/N)} \text{, where } n = 0, 1, \ldots, (N-1), \tag{2.11}$$

$$x(t_m) = \frac{1}{N} \sum_{n=0}^{N-1} X(n \Delta \omega) e^{i(mn/N)} \text{, where } m = 0, 1, \ldots, (N-1). \tag{2.12}$$

The DFT operation is usually performed using the Fast Fourier Transform (FFT) algorithm, developed by Cooley and Tukey (1965).

2.2.4 Frequency Response Function

Instead of performing the convolution of the IRF and the input force, the response of an SDOF system can be obtained in the frequency domain by simply multiplying the Fourier Transform of the forcing function, $F(\omega)$, and the complex frequency response function (FRF), $H(\omega)$.

$$U(\omega) = H(\omega) \cdot F(\omega) \qquad [2.13]$$

The FRF of an SDOF oscillator is represented by

$$H(\omega) = \frac{1/k}{\left[1 - (\omega/\omega_n)^2\right] + i\left[2\xi(\omega/\omega_n)\right]}. \qquad [2.14]$$

From Equation 2.13, it is clear that the FRF acts as a filter (or transfer function) between the input $F(\omega)$ and the output $U(\omega)$, as shown in Figure 1.

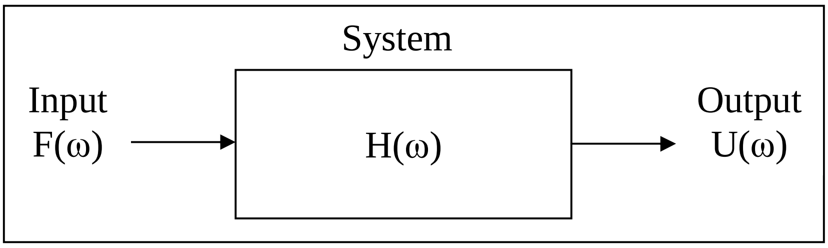

Figure 1: Illustration of the relationship between input, output, and FRF

Similarly to the IRF, the FRF contains all the information about the system dynamics and is independent of the forcing function. In fact, the IRF and FRF are Fourier pairs. Further, we can say that the convolution of two functions in the time domain is equivalent to the multiplication of their Fourier Transforms in the frequency domain (see Equations 2.2 and 2.13).

2.3 Response spectra

Typically, in design, the temporal variation of the various response parameters is of little interest; rather, designers are concerned with their maximum values. A response spectrum is a plot of the maximum response to a *specified excitation* for all SDOF systems. Typically, they are presented for a given level of damping (e.g. 5% damped). Further, since most buildings are considered lightly damped (typically of the order of 3% to 5% of critical damping), it is common to neglect the difference between the undamped and damped natural frequencies in the development of response spectra.

In earthquake engineering, three important response spectra are widely used: the displacement, pseudo-velocity and pseudo-acceleration response spectra denoted respectively, S_d, S_v, and S_a. The displacement response spectrum is a plot of the maximum relative displacement of all SDOF systems to a particular excitation. It can be obtained using the convolution integral.

For a base motion problem, with ground acceleration $\ddot{u}_g(t)$ and relative displacement $u(t)$, the equation of motion becomes

$$m\ddot{u}(t) + c\dot{u}(t) + ku(t) = -m\ddot{u}_g(t), \qquad [2.15]$$

which leads to the following solution

$$u(t) = \frac{1}{\omega_n}\int_0^t \ddot{u}_g(\tau)\, e^{-\xi\omega_n(t-\tau)} \sin\omega(t-\tau)\, d\tau. \qquad [2.16]$$

If the maximum value of $u(t)$ for a particular oscillator occurs at time t_m, then the spectral displacement (corresponding to the natural frequency of the oscillator) is

$$S_d(\omega_n, \xi) = u_{\max} = u(t_m) = \frac{1}{\omega_n}\int_0^{t_m} \ddot{u}_g(\tau)\, e^{-\xi\omega_n(t_m-\tau)} \sin\omega(t_m-\tau)\, d\tau. \qquad [2.17]$$

In most cases, this integral is difficult, if not impossible, to solve analytically, and a numerical solution is used. The pseudo-velocity and pseudo-acceleration spectra are obtained simply by multiplying the displacement response spectrum by the appropriate power of the undamped natural frequency.

$$\begin{aligned} S_v(\omega_n, \xi) &= \omega_n\, S_d(\omega_n, \xi) \\ S_a(\omega_n, \xi) &= \omega_n\, S_v(\omega_n, \xi) = \omega_n^{\,2}\, S_d(\omega_n, \xi) \end{aligned} \qquad [2.18]$$

These are referred to as pseudo- spectra because, unlike the displacement response spectrum, they do not truly represent the maximum velocity or displacement of an oscillator having given period and damping to a particular ground motion. Only in the case of an undamped system would the pseudo- spectra correspond to the true relative velocity and absolute acceleration response spectra. However, since most buildings are only lightly damped, the pseudo- spectra are an adequate estimate of the true response spectra. This type of simplification also allows the three response spectra to be plotted on the same scale, sometimes referred to as a tripartite representation of ground motion.

2.4 Base shear

The maximum base shear in a linear elastic SDOF oscillator is

$$V_{\max} = k\, u_{\max} = k\, S_d(\omega_n, \xi) = \frac{k}{\omega_n^{\,2}} S_a(\omega_n, \xi) = m S_a(\omega_n, \xi) = \frac{S_a(\omega_n, \xi)}{g} W \qquad [2.19]$$

This illustrates the usefulness of the pseudo-acceleration response spectrum: once it is known only the weight (W) of the SDOF system is needed to estimate the maximum elastic base shear that can be expected during a particular ground motion. This equation is the basis of the lateral seismic force requirements in most building codes.

2.5 Response of linear MDOF systems under general excitation

In most cases, however, assuming that the entire mass, stiffness and damping of a building can be lumped at one point moving along only one degree of freedom is an unacceptable simplification. Therefore, most buildings are better modeled by a multiple degree-of-freedom (MDOF) system, rather than an SDOF system. In an MDOF system, the mass, stiffness and damping are not concentrated at a single point, but distributed along the height, width and length of the building at discrete points where the dynamic degrees of freedom are assigned. In such instances, it is common to use a lumped parameter approach, whereby mass, stiffness and damping are lumped at each floor level. The equation of motion for a lumped parameter, viscously damped, elastic N-degree of freedom system, subject to general dynamic excitation is

$$[M]\{\ddot{u}(t)\}+[C]\{\dot{u}(t)\}+[K]\{u(t)\}=\{F(t)\}. \qquad [2.20]$$

2.5.1 Mode-superposition method

In general, the coefficient matrices in the above equation contain non-zero off-diagonal terms (often referred to as coupling terms). Therefore, solving the above equations would involve the simultaneous solution of N equations in N unknowns. The mode-superposition method is a technique used to reduce these coupled linear equations into a set of uncoupled equations by making use of the undamped natural modes of the structure, which define a new coordinate system (Craig and Kurdila 2006).

The first step of the mode-superposition method is to find the undamped natural modes of the N-DOF system by solving an eigenproblem. Numerical procedures to find the modes are available in any structural dynamics textbook. For an N-DOF system, there are N modes of vibration. The modes of vibration can then be combined in the NxN modal matrix.

$$[\Phi]=\left[\{\varphi_1\}\ \{\varphi_2\}\ \{\varphi_3\}\ldots\{\varphi_N\}\right] \qquad [2.21]$$

If we now assume that the displacement of the system can be represented by

$$\{u(t)\}=[\Phi]\{q(t)\}, \qquad [2.22]$$

where $\{q(t)\}$ is the vector of modal coordinates (notice that this is essentially a separation of variables, where $[\Phi]$ and $\{q(t)\}$ respectively capture the spatial and temporal variation of the response), then the equation of motion can (eventually) be represented by

$$[\Phi]^T[M][\Phi]\{\ddot{q}(t)\} + [\Phi]^T[C][\Phi]\{\dot{q}(t)\} + [\Phi]^T[K][\Phi]\{q(t)\} = [\Phi]^T\{F(t)\}. \qquad [2.23]$$

Because of the orthogonality properties of mode shapes (Craig and Kurdila 2006), the modal mass matrix is diagonal with values of M_r corresponding to the r^{th} mode. Similarly, the modal stiffness matrix is diagonal with values of $\omega_r^2 M_r$ corresponding to the r^{th} mode.

$$[\Phi]^T[M][\Phi] = diag\left[M_r\right] \qquad [2.24]$$

$$[\Phi]^T[K][\Phi] = diag\left[\omega_r^2 M_r\right] \qquad [2.25]$$

As for the damping matrix, it will most likely not be diagonalized by the modal matrix. However, it is common to specify an overall structural damping ratio, rather than localized element damping factors. One of the more common ways of doing this is to assume modal damping, which assumes that the modal matrix diagonalizes the damping matrix, such that

$$[\Phi]^T[C][\Phi] = diag\left[2\xi_r\omega_r M_r\right], \qquad [2.26]$$

where ξ_r is the modal damping ratio for mode r.

With the above assumptions, the equations of motion are fully uncoupled, and can thus be solved independently. For mode r,

$$M_r\ddot{q}_r + 2\xi_r\omega_r M_r\dot{q}_r + \omega_r^2 M_r q_r = \{\phi_r\}^T\{F(t)\}, \qquad [2.27]$$

where $M_r = \{\phi_r\}^T[M]\{\phi_r\}$ is the modal mass for mode r. Similarly to Equation 2.1, this equation can be solved using the convolution integral.

$$q_r(t) = \frac{1}{M_r\,\omega_r}\int_0^t \{\phi_r\}^T\{F(t)\}e^{-\xi_r\omega_r(t-\tau)}\sin\omega_r(t-\tau)\,d\tau \qquad [2.28]$$

Thus, the mode-superposition method allows the independent calculation of the contributions of each mode to the overall motion of the structure. These modal contributions can then be superimposed to recover the total motion of the structure.

$$\{u(t)\} = [\Phi]\{q(t)\} = \sum_{r=1}^{N} \{\phi_r\} q_r(t) \qquad [2.29]$$

2.5.2 *Frequency domain response of MDOF systems under general excitation*

Similarly to SDOF systems, the input at a particular DOF can be related to the output at another DOF by an FRF, which contains the dynamic properties of the system. But clearly, for MDOF systems, a given input at a particular DOF will not cause the same output at all DOFs. Similarly, the output at a particular DOF will not be the same if the exact same input is applied at different DOFs. Therefore, a different FRF will exist between each input and each output. For an *N*-DOF system with inputs at *m* DOFs, the different FRFs can be represented by an *N*x*m* FRF matrix. Thus, element $H_{jk}(\omega)$ of the FRF matrix represents the relationship between the output at DOF *j*, $U_j(\omega)$, and the input at DOF *k*, $F_k(\omega)$.

$$U_j(\omega) = H_{jk}(\omega) \cdot F_k(\omega) \qquad [2.30]$$

$$H_{jk}(\omega) = \sum_{r=1}^{N} \frac{\phi_{jr}\,\phi_{kr}}{K_r} \frac{1}{\left[1-(\omega/\omega_r)^2\right] + i\left[2\,\xi_r\,(\omega/\omega_r)\right]}, \qquad [2.31]$$

where $K_r = \{\phi_r\}^T [K] \{\phi_r\}$ is the modal stiffness for mode *r*,

ϕ_{jr} is the element of the r^{th} mode corresponding to DOF *j*, and

ϕ_{kr} is the element of the r^{th} mode corresponding to DOF *k*.

Alternatively, the FRF can be expressed in pole-residue form. This representation is widely used in Experimental Modal Analysis.

$$H_{jk}(\omega) = \sum_{r=1}^{N} \left(\frac{Q_r\,\phi_{jr}\,\phi_{kr}}{i\,\omega_r - \lambda_r} + \frac{Q_r^{\,*}\,\phi_{jr}^{\,*}\,\phi_{kr}^{\,*}}{i\,\omega_r - \lambda_r^{\,*}} \right) , \qquad [2.32]$$

where $\lambda_r = -\xi_r\,\omega_r + i\,\omega_r\sqrt{1-\xi_r^{\,2}}$ is the complex pole of mode *r*, and

$$Q_r = -\frac{i}{2\,M_r\,\omega_r\sqrt{1-\xi_r^{\,2}}}$$

Regardless of the form of the FRF, Equation 2.13 still holds for MDOF systems, only the terms in the expression are vectors or matrices: $U(\omega)$ is the *N*x1 vector of outputs at the *N* DOFs; $F(\omega)$ is the *m*x1 vector of inputs at the *m* DOFs; and $H(\omega)$ is the *N*x*m* matrix containing the FRFs between all the inputs and outputs.

$$\underset{Nx1}{\{U(\omega)\}} = \underset{Nxm}{[H(\omega)]} \cdot \underset{mx1}{\{F(\omega)\}} \qquad [2.33]$$

Let us now consider the spectral density matrices of the input and output signals. The spectral density is a measure of the energy content of a signal (or of a pair of signals) per unit frequency.

$$\underset{NxN}{[P_{uu}(\omega)]} = E\left[\underset{Nx1}{\{U(\omega)\}} \cdot \underset{1xN}{\{U(\omega)\}^H}\right], \qquad [2.34]$$

$$\underset{mxm}{[P_{ff}(\omega)]} = E\left[\underset{mx1}{\{F(\omega)\}} \cdot \underset{1xm}{\{F(\omega)\}^H}\right], \qquad [2.35]$$

where E is the expected value operator. From the above equations, and dropping the notation referring to frequency for conciseness, the following relationship between the input and output spectral density matrices can be obtained.

$$\underset{NxN}{[P_{uu}]} = \underset{Nxm}{[H]} \cdot \underset{mxm}{[P_{ff}]} \cdot \underset{mxN}{[H]^H} \qquad [2.36]$$

2.5.3 Response of MDOF systems to earthquake ground motion

The equation of motion that describes the response of an MDOF system to base excitation is

$$[M]\{\ddot{u}(t)\} + [C]\{\dot{u}(t)\} + [K]\{u(t)\} = [M]\{1\}\ddot{u}_g(t), \qquad [2.37]$$

where $\{1\}$ is an Nx1 vector of 1's when only translational motion is considered.

By making use of the mode-superposition method, these equations can again be uncoupled.

$$M_r\ddot{q}_r + 2\xi_r\omega_r M_r\dot{q}_r + \omega_r^2 M_r q_r = \{\phi_r\}^T[M]\{1\}\ddot{u}_g(t) \qquad [2.38]$$

This equation is very similar to Equation 2.27, and thus leads to the following solution:

$$q_r(t) = \frac{\{\phi\}^T[M]\{1\}}{M_r\omega_r}\int_0^t \ddot{u}_g(t)e^{-\xi_r\omega_r(t-\tau)}\sin\omega_r(t-\tau)d\tau. \qquad [2.39]$$

The relative displacement vector, containing the displacements of the different DOFs relative to the ground, as a function of time, can then be recovered by adding the contributions of all the vibration modes.

$$\{u(t)\} = \sum_{r=1}^{N} \{\phi_r\} q_r(t) \qquad [2.40]$$

However, in most cases the integration of the ground motion to obtain the time histories of the modal responses is an unreasonably demanding procedure. As in the case of SDOF systems, it is common to work with response spectra to obtain the maximum modal responses.

$$|u_r|_{\max} = |\phi_r| \cdot \frac{\left|\{\phi\}^T [M]\{1\}\right|}{M_r \omega_r} \cdot S_v(\omega_r, \xi_r) \qquad [2.41]$$

However, the maxima of the different modes generally will not occur simultaneously. Therefore, simply adding the maximum values from each mode would lead to overly conservative estimates of the displacements, velocities, accelerations, etc. To circumvent this problem, it is common to use a Square Root of the Sum of Squares (SRSS) approach to combine the modal contributions.

$$|u|_{\max} = \sqrt{\sum_{r=1}^{N} \left(|u_r|_{\max}\right)^2} \qquad [2.42]$$

This yields more realistic maximum values, as long as the system does not contain closely-spaced modes. Other modal combination methods exist, such as the Complete Quadrature Combination (CQC) and the Closely Spaced Mode (CSM) method. All of these methods aim to provide an estimate of the expected value of the maximum response.

3. Overview of seismic design provisions in Canada

Seismic design was a mandatory consideration from the very first edition of the National Building Code of Canada (NBCC) in 1941. Periodic changes were made to the seismic design provisions of the NBCC to reflect the advances in knowledge. The purpose is to develop simple guidelines, which provide a reasonable level of protection of life safety throughout the country.

The discussion below summarizes the evolution of seismic design requirements in the National Building Code of Canada, as well as the underlying research which lead to these changes.

3.1 NBCC 1941

The first edition of the National Building Code of Canada was published in 1941. In this edition, it was recognized that earthquakes had the potential to cause extensive building damage in certain parts of the country. In the body of the Code itself, only a brief sentence was included which stated that, in regions where significant earthquakes were probable, every structure, and part thereof, should be designed to resist the horizontal forces induced by such an earthquake (NBCC 1941).

A method of calculating the forces due to earthquake ground motion was included in the Appendix. Each portion of the structure was to be designed for a force

$$F = C \cdot W, \tag{3.1}$$

where W consisted of the dead load and half of the live load of the portion under consideration and C was a constant which depended on the component under consideration.

By today's standards, this would of course be grossly inadequate; however this Code represented a first attempt to standardize the calculation of design loads in general, and seismic design loads in particular.

3.2 NBCC 1953

In this edition, seismic design loads were included in the main body of the Code, rather than in the Appendix. Further, an earthquake probability map was included in the climatic information section. This map, prepared by the Dominion Observatory Department of Mines and Technical Surveys, contained four zones, which represented a qualitative estimation of the damage that could be expected from future earthquakes, based on historical seismic activity (NBCC 1953).

The equation for calculating seismic design loads was the same as in the 1941 edition, though a few changes were made to the values of C. The base shear calculated from that equation represented the design load for zone 1, which had to be doubled for zone 2 and quadrupled for zone 3 (consideration of seismic loads was not required for zone 0). In addition, a few extra sentences were included addressing the importance of the symmetrical layout of braces with respect to the center of mass of the structure (to limit torsional effects), the application of design loads at each floor level, and structural separation to avoid pounding.

It is also interesting to note that load combinations were introduced in this edition. That is, it was necessary to consider simultaneously the effects of all lateral and vertical loading combinations in the Working Stress Design approach (though the probabilistic combination of these loads was only introduced later); however it was not necessary to consider earthquake and wind loads simultaneously.

3.3 NBCC 1960

The only major change that occurred in the 1960 edition was that dynamic analysis, by a professional competent in this field, was formally recognized as an alternative method to calculate seismic design loads (NBCC 1960). This alternative remains in the NBCC to this day. In fact, in the NBCC 2005, it is the preferred approach.

3.4 NBCC 1965

Significant changes were made in the 1965 edition to account for five main factors that influence the seismic performance of structures: location, construction, function, foundation, and dynamic properties (NBCC 1965b).

Seismic analysis was to be performed by dynamic analysis or using the Equivalent Static Force Procedure (ESFP). In the ESFP, the design base shear was calculated using the equation

$$V = K \cdot W \,, \qquad [3.2]$$

where W was the total weight of the structure (including all building materials and components, as well as the full design occupancy load) and K was calculated using

$$K = R \cdot C \cdot I \cdot F \cdot S \,, \qquad [3.3]$$

where R was an earthquake factor (a measure of estimated intensity of seismic forces)
C was a factor that reflected the type of construction
I was an importance factor, which reflected the importance of the building
F was a factor to account for foundation conditions
S was a factor that represented the shape of the design acceleration response spectrum.

In contrast to the equation in previous Codes, it is clear from the form of this equation that an attempt was made to recognize the effects of various phenomena on the maximum base shear expected during the design earthquake. These are discussed below.

3.4.1 Hazard

In 1965, the seismic hazard was still based on the four-zone hazard map introduced in the 1953 edition and based on a qualitative estimation of historical seismic activity in Canada. In contrast to the 1960 edition however, seismic hazard was reflected explicitly in the base shear equation through an earthquake factor, R, rather than through a multiplication of the zone 1 base shear for zones 2 and 3.

3.4.2 Type of Construction

It has long been accepted that the type of construction has a significant effect on the behavior of structures during earthquakes. Buildings having significant ductility and inelastic energy dissipation capacity performed very well in past earthquakes, even in cases where significant damage was reported on other types of structures (NBCC 1965a). In the 1965 edition of the NBCC, this was addressed by multiplying the elastic base shear by a factor C, ranging from 0.75 for steel or reinforced concrete buildings, with moment-resisting connections, with floors and roof sufficiently strong and stiff to distribute lateral forces to the lateral load resisting elements, and in which the frame alone was able to carry at least fifty percent of the design shears or in which shear walls were able to carry design shears in a ductile manner; to 1.25, for all other buildings. This factor was based on the best judgment of experts at the time, rather than on sophisticated analyses of the actual ductility of different types of lateral force resisting systems.

3.4.3 Building Importance

The idea behind the importance factor was, and still is, simply to make the Code requirements more stringent for structures that are expected to be operational after an important earthquake (hospitals, emergency shelters, etc.), in order to provide a larger margin of safety in their design.

3.4.4 Foundation Effects

The foundation factor, F, was meant to account for the amplification of seismic ground motion in soft soils, and the fact that most building damage in past earthquakes had occurred on soft soil sites (NBCC 1965b). Since little data was available at the time to rationally quantify the behavior of soils during seismic ground motion (soil dynamics is a fairly young discipline), a judgment factor was adopted to amplify the base shear when the underlying soil was considered to be "highly compressible" (NBCC 1965a).

3.4.5 Spectral Effects

Earthquakes do not excite all structures equally because of their frequency content, as reflected in the notion of a response spectrum (see section 2.3). In 1965, an attempt was made to account for the spectral variation of design forces by specifying a design response spectrum based on the number of storeys (rather than on the actual building period). The shape of the response spectrum was captured in the factor

$$S = \frac{0.25}{9 + N}, \qquad [3.4]$$

where N was the number of storeys. Though it is not clear how this formula was developed, Supplement No. 3 of the NBCC 1965 states that "the seismic coefficient in the National Building Code gives a first order approximation" to the design response spectrum (NBCC 1965b).

3.4.6 Distribution of Seismic Forces

In the ESFP, the base shear calculated by Equation 3.2 was then distributed along the building height based on an approximately triangular variation of loads (triangular if storey weights are identical), with the apex at the base. This distribution, first suggested by Anderson et al. (1952), who had investigated the deflections of a uniform cantilever due to shear deflection only and to flexural deflection only, was based on the assumption of fundamental mode response only.

$$F_x = V \cdot \frac{W_x h_x}{\sum_{i=1}^{N} W_i h_i} \ , \qquad [3.5]$$

where x indicates the storey under consideration.

This simple static lateral force distribution was found to be reasonable to represent the inertia forces induced by earthquakes at the centroid of floors for building structures having a height to width ratio less than 3 or a fundamental period less than 1 second (NBCC 1970b). However, the Code allowed the ESFP to be used for all buildings.

3.5 NBCC 1970

In this edition, the design base shear was calculated using

$$V = \frac{1}{4} \cdot R \cdot K \cdot C \cdot I \cdot F \cdot W \, , \qquad [3.6]$$

where R was a seismic regionalization factor
K was a factor that reflected the type of structural system
C was a factor representing the shape of the response spectrum (similar to S in 1965)

The weight of the structure, W, was explicitly required to include 25% of the design snow load, in addition to the full weight of all building components and the entire design use and occupancy load (NBCC 1970a).

3.5.1 Hazard

The seismic hazard was revised for this edition of the NBCC, based on new seismic hazard maps from the Geological Survey of Canada. These maps still contained four zones; however the boundaries were based on peak ground acceleration (PGA) at a 0.01 annual probability of exceedance. These were developed using the Gumbel extreme-value method using PGA values from past earthquakes in and around Canada between 1900 and 1963 (Heidebrecht 1995). This was clearly an improvement over earlier maps, since PGA was now used as an indicator of damage potential in a region, rather than simply using a qualitative assessment of seismic hazard.

3.5.2 Type of Construction

The factor C included in the 1965 edition to account for the performance of certain types of structural systems in past earthquakes was replaced by a factor K, serving exactly the same purpose. However, more types of structural systems were included, and the value of K ranged from 0.67 for ductile moment-resisting frame buildings to 3.00 for certain types of elevated tanks.

3.5.3 Spectral Effects

The design response spectrum in the 1970 edition, denoted C, was changed from that in the 1965 edition, denoted S.

$$C = 0.10 \quad \text{for single- or two- storey buildings, and} \tag{3.7}$$

$$C = \frac{0.05}{\sqrt[3]{T}} \leq 0.10 \quad \text{for all other buildings,} \tag{3.8}$$

where T was the fundamental period of the structure. This was the first attempt to explicitly recognize the importance of the fundamental period in calculating seismic design loads. This response spectrum was adopted based on recommendations from the Structural Engineers Association of California (SEAOC) Seismology Committee (NBCC 1970b). Thus, the calculation of base shear according to the NBCC 1970 was based on a period-dependent design response spectrum, which provides a better representation of the governing dynamics. This rational approach to the calculation of seismic design forces remains to this day, though significant changes have been made to the way in which the design spectrum is obtained.

This approach required the calculation of the fundamental period of the structure in each principal direction. Since this is a quantity that cannot be exactly determined before a structure is built, the following empirical formulae were suggested.

$$T = \frac{0.05h}{\sqrt{D}} \quad \text{for all buildings, except} \tag{3.9}$$

$$T = 0.1N \quad \text{for all buildings in which moment resisting frames resist 100\% of the seismic design loads,} \qquad [3.10]$$

where h was the height of the building (in feet), and
D was the length of the building (in feet) in the direction parallel to the applied forces.

The first period formula was based mainly on vibration measurements conducted by the U.S. Coast and Geodetic Survey (USCGS) in 430 buildings and 42 elevated water tanks prior to July 1949 (Anderson et al. 1952), but it is unclear what type of vibration testing methods were used. Though significant scatter was observed in the data, the authors determined that approximately 80% of observed fundamental building periods lied above the values obtained from the above equation. This was deemed conservative since design loads decreased with increasing period based on the shape of the design response spectrum.

3.5.4 Distribution of Seismic Forces and Higher Mode Effects

Bustamante (1965) compared the shear force and overturning moment distributions obtained from the ESFP of the SEAOC provisions to those obtained from modal analyses for 11 real buildings and 20 imaginary buildings whose mass and stiffness distributions were selected to emphasize the differences between the ESFP and dynamic analyses. He showed that storey shears in the upper levels obtained from the ESFP were often lower than their dynamic equivalents, particularly in slender buildings having long fundamental periods, because of the effects of higher modes. He suggested assigning an additional force at the top storey of the building in the ESFP to increase the shears in the upper levels. In the NBCC, instead, a portion of the design base shear was assigned to the top storey when the ratio of the height, h, to the length of the lateral load-resisting system, D_s, was greater than 3.

$$F_t = 0.004V\left(\frac{h}{D_s}\right)^2 \leq 0.15V \qquad [3.11]$$

The remainder $(V - F_t)$ was distributed along the building height according to the same distribution as previously assumed.

$$F_x = (V - F_t)\cdot\frac{W_x h_x}{\sum_{i=1}^{N} W_i h_i} \qquad [3.12]$$

However, the overturning moments resulting from this distribution of lateral forces were found to overestimate the true overturning moments, since higher mode effects tend to reduce the overturning moments (Bustamante 1965). Therefore, a base overturning moment reduction factor, J, was introduced.

$$J = 0.5 + \frac{0.25}{\sqrt[3]{T^2}} \leq 1.0 \qquad [3.13]$$

Storey-level overturning moments were also reduced in a similar manner.

3.5.5 Interstorey Drift

In this edition, an additional clause was added requiring the consideration of interstorey drift in accordance with accepted practice. The main purposes of this provision were to ensure the comfort of occupants, limit damage to nonstructural components, and in some cases avoid pounding between adjacent buildings. Though the clause itself seemed vague, Supplement 4 (NBCC 1970b) provided some useful guidelines. Namely, it suggested that the interstorey drift be limited to 0.005 times the storey height, and that drift did not need to be considered for buildings less than 13 storeys in height. It should be noted that there were no guidelines to help in the calculation of drift. It is assumed that the storey drifts were to be calculated using the equivalent static loads in an elastic analysis, a procedure that was rectified in the 1975 edition.

3.6 NBCC 1975

It is important to note that in this edition of the NBCC, Limit States Design was introduced as an alternative to Working Stress Design, which was the norm until then (NBCC 1975a; NBCC 1975b). Limit States Design is a probabilistic approach to structural design, which accounts for the variability of the different variables used in determining design loads and design resistances. It thus provides a better indication of structural reliability than does the Working Stress Design approach.

The base shear equation for the NBCC 1975 was slightly changed to reflect a change in the determination of the seismic hazard. It had the form:

$$V = A \cdot S \cdot K \cdot I \cdot F \cdot W, \qquad [3.14]$$

where A was the design ground acceleration at a 0.01 annual probability of exceedance, and
S was a seismic response factor (formerly C),

Though it may appear that this edition of the NBCC relied on a different hazard map than the 1970 version, in fact it did not. It was the same map, with four zones whose boundaries were based on peak ground acceleration values at a 0.01 annual probability of exceedance. The difference lies in the fact that the 1970 version used a non-dimensional factor R, ranging from 0 to 4, which reflected the relative seismicity of the different zones; whereas the 1975 version used the zonal PGA value directly in the base shear equation. This was an important improvement as it provided a more rational basis for the calculation of the seismic design forces.

As mentioned above, clearer guidelines to calculate interstorey deflections were included in this edition. The storey drifts obtained from an elastic analysis using the equivalent static loads were to be multiplied by 3 to obtain more realistic values of the displacements. This requirement was included to permit some plastic deformation during the design ground motion.

3.7 NBCC 1980

No significant changes were made to the seismic provisions of the 1977 edition of the Code (NBCC 1977), while the main change in the NBCC 1980 was a shift from imperial to SI units (NBCC 1980a). As a result, the form of many equations had to be changed to account for unit conversions.

The formula to determine the fundamental period for structures other than moment-resisting frames was changed to

$$T = 0.09\frac{h}{\sqrt{D}}. \qquad [3.15]$$

However, the Rayleigh method was explicitly introduced as an alternative to calculate the fundamental period of structures, the details of this method being presented in the supplement (NBCC 1980b).

Also, a limit was imposed on the base shear obtained from a dynamic analysis. This limit was set to 90% of the base shear obtained by the ESFP.

3.8 NBCC 1985

Significant changes were made in this edition of the NBCC to incorporate a new seismic hazard map, which mapped the peak ground velocity (PGV), in addition to the peak ground acceleration (PGA).

The equation to determine the design base shear was changed to

$$V = v \cdot S \cdot K \cdot I \cdot F \cdot W, \qquad [3.16]$$

where v was the zonal velocity ratio.

It is clear that the Code moved from an equation based on zonal peak ground acceleration to one based on zonal peak ground velocity. However, the zonal acceleration was still taken into account indirectly in the seismic response factor (NBCC 1985a). The reason for this change was that PGA is a reasonable indicator of the damage potential of an earthquake for structures in the short period range (near 0.2s). However, most medium- to high- rise buildings have fundamental periods greater than 0.5s, and their seismic behavior depends more on the velocity of the ground motion (Heidebrecht 1995). Thus, peak ground velocity (PGV) is a better indicator of damage potential for buildings in the intermediate period range (0.5s to 1s).

3.8.1 Hazard

As mentioned previously, a new hazard map was used in the formulation of the NBCC 1985 seismic design provisions. This map was developed using the Cornell-McGuire method (Cornell 1968; McGuire 1976), rather than the extreme-value method which was previously used, applied to a data set that included not only the historical earthquake record, but also some geological and tectonic information (NBCC 1985b). New ground motion attenuation relations, developed by Hasegawa et al. (1981), were used in the development of these maps. Finally, in addition to the peak ground acceleration, peak ground velocity was also mapped, both at a probability of exceedance of ten percent in fifty yeas, rather than the 0.01 annual probability of exceedance previously used.

The country was divided into seven acceleration- and velocity- related regions (ranging from 0 to 6) with boundaries based on the PGA and PGV values at a probability of exceedance of 10% in fifty years.

3.8.2 Spectral Effects

The value of the seismic response factor was reduced significantly in this edition, as compared to the NBCC 1980, based on calibration of 1985 base shears to 1980 levels (Heidebrecht et al. 1983).

It was realized that a single parameter (PGA or PGV) was insufficient to represent damage potential for the entire period range, but the ratio of PGA to PGV was found to adequately represent the frequency content of seismic ground motion (Heidebrecht 1995). Thus, the shape of the response spectrum was modified to account for the levels of acceleration- and velocity-related seismicity, Z_a and Z_v, respectively; whereas in previous versions, it was solely based on the period (or the number of storeys).

In this edition, a limit was also imposed on the period calculated by the Rayleigh method, such that it not exceed the period calculated by the Code formulae by more than 20%. This represented a change in approach from the previous Code, in which a limit was instead imposed on the base shear obtained using a different period than that provided by the Code formulae (see NBCC 1980).

3.8.3 Distribution of Seismic Forces

It was recognized that dynamic analysis provides a better way of determining the seismic force distribution than does the ESFP. Thus, the NBCC 1985 recognized that distributing the base shear obtained by the ESFP using a modal analysis was a valid alternative for determining the distribution of seismic design loads, and adequate methods of analysis were included in the Appendix.

3.9 NBCC 1990

In this edition of the Code, an attempt was made to provide a more rational basis for the calculation of the design base shear. The elastic base shear, V_e, was determined using the same equation as the 1985 edition, but without the *K* factor (recall that this was a judgment factor reflecting the general performance of the different types of lateral load resisting systems in past earthquakes):

$$V_e = v \cdot S \cdot I \cdot F \cdot W. \tag{3.17}$$

The elastic base shear was then divided by a force modification factor, *R*, and multiplied by a calibration constant, *U*, having a value of 0.6, which was a substitute for the previous K factor approach (NBCC 1990a).

$$V = \frac{V_e}{R} \cdot U \tag{3.18}$$

3.9.1 Type of Construction

The force modification factor was meant to account for the energy absorption capacity of the structural system through damping and inelastic deformation capacity (ductility). It encompassed a structure's energy absorption capacity; structural redundancy; the capacity to undergo inelastic cyclic deformations; and the fact that damping typically increases with the level of excitation. *U* was a calibration factor intended to maintain similar base shears between the 1985 and 1990 editions of the NBCC, on average, across the country. (NBCC 1990b)

3.9.2 Distribution of Seismic Forces and Higher Mode Effects

The portion of the base shear assigned to the top storey was changed to

$$F_t = 0.07 \cdot T \cdot V \leq 0.25V, \tag{3.19}$$

where T was the fundamental period of the building in the direction under consideration. This change reflected the idea that higher mode contributions were a direct function of the fundamental period, rather than the building slenderness. Thus, the revised equation was considered to be a more rational way to incorporate higher mode effects than the equations based on building slenderness in previous Codes (NBCC 1990b).

3.9.3 Interstorey Drift

Since the force modification factor accounted for the plastic deformation capacity of the system, it was decided to use this parameter directly in the calculation of interstorey drifts. Rather than the somewhat arbitrary factor of 3 included in previous editions, the elastic interstorey drift needed to be multiplied by R to obtain realistic estimates of the interstorey displacements. Further, limits of 0.01 and 0.02 times the storey height were imposed for post-disaster buildings and all other buildings, respectively, in contrast to previous editions where similar limits were simply suggestions.

3.10 NBCC 1995

The main changes in this edition were the introduction of alternative period formulae for moment-resisting frames and the formal treatment of *P-delta* effects (NBCC 1995a). Two alternative formulae were suggested to calculate the fundamental period of steel and reinforced concrete (RC) moment-resisting frames (MRF)

$$T = 0.085 \cdot h_n^{3/4} \text{ for steel MRF, and} \qquad [3.20]$$

$$T = 0.075 \cdot h_n^{3/4} \text{ for RC MRF.} \qquad [3.21]$$

The rationale for these formulae is discussed further in Section 4. Also, it had long been recognized that the additional moments created by the lateral deflections of the structure reduced the capacity of structures to resist lateral seismic loads (NBCC 1995b). This phenomenon, commonly called *P-delta* effect, was addressed by multiplying storey forces, shears, overturning moments and torsional moments (but not displacements) by a stability factor.

3.11 NBCC 2005

Many changes were made to the seismic design provisions between the 1995 and 2005 versions of the NBCC, including a new way of characterizing seismic hazard, changes in the fundamental period formulae, introduction of period- and intensity- related site effects, separation of ductility and overstrength force modification factors, and the use of an additional higher mode factor. Further, dynamic analysis is now the preferred method, except that the ESFP can be used in certain circumstances (NBCC 2005a). The major changes, as well as the research that lead to these changes, will be discussed here.

The ESFP is now restricted to:

a) Structures in low seismicity areas, or
b) Regular structures of height less than 60m and fundamental period less than 2s, or
c) Structures having certain types of irregularity (these are defined in the Code), of height less than 20m and fundamental period less than 0.5s. (NBCC 2005a)

In any of these cases, the design base shear may be calculated using

$$V = \frac{S(T) \cdot M_v \cdot I_E \cdot W}{R_d \cdot R_o}, \qquad [3.22]$$

where $S(T)$ is obtained from the modified Uniform Hazard Spectrum (UHS)
M_v is a higher mode factor
I_E is the earthquake importance factor
R_d is the ductility-related force modification factor
R_o is the overstrength-related force modification factor.

Certain restrictions are imposed on the value of V to ensure a minimum force level, as well as to avoid undue conservatism. It is also interesting to note that the ESFP can no longer be systematically applied in Montreal.

3.11.1 Hazard

As mentioned previously, a new seismic hazard map was created for this edition of the NBCC. In previous Codes, a map of PGA and PGV values was used. These values were then scaled based on an assumed response spectrum to obtain the spectral variation (or the frequency content) of the ground motion. This however did not adequately capture the spectral variation, and did not ensure uniform reliability for all building periods. Therefore, it was decided to create a map based on 5% damped spectral acceleration ordinates at specific periods, with a uniform probability of exceedance of 2% in 50 years (return period of approximately 2500 years) and a median confidence level (NBCC 2005b). This is therefore referred to as a Uniform Hazard Spectrum (UHS).

This map was developed using the Cornell-McGuire method (Adams and Atkinson 2003). Two source zone models denoted *H* and *R*, were used to represent the spatial distribution of seismic activity in Canada. Within each of these zones, the probability of an event was assumed constant (uniformly distributed), and the temporal variation (or magnitude-recurrence relations) was based on historical seismic activity. These models allowed the estimation of the probability of occurrence of seismic events as a function of geographic location in Canada. However, these events affect a large area by virtue of the propagation of seismic waves. It was therefore necessary to model the propagation of seismic waves as well.

To address this, ground motion attenuation relations were required to transform a specific earthquake – i.e. an earthquake of a certain magnitude within a given source zone, having a certain probability of occurrence – to a ground motion parameter at a specific site (in this case, a spectral acceleration ordinate). In this case, the median (50^{th} percentile) spectral acceleration ordinate at a site, as well as the probabilistic distribution about the median value, was determined based on earthquake magnitude and distance from the source.

This however represents the median spectral acceleration ordinate, at a given site and for a specific period, that results from a *specific* earthquake. To calculate the probability of exceeding a certain ground motion at a site, the hazard contributions from earthquakes of all magnitudes and distances, from all source zones, were then integrated. These calculations of probability of exceedance were repeated for different target ground motion amplitudes, and the values were interpolated to achieve the target probability of exceedance of 2% in 50 years. Finally, this was done for different periods, and for the two source zone models, and a "robust approach" was used, in which the more conservative value from the two models was used. (Adams and Atkinson 2003)

3.11.2 Type of Construction

As mentioned previously, the effects of ductility and overstrength were separated and explicitly accounted for in the base shear formula in this edition of the NBCC. The ductility-related force modification factor, R_d, essentially replaces the force-modification factor, R, in previous Codes. The overstrength-related force modification factor, R_o, was included to account for the fact that the lateral resistance of structures is typically greater than that assumed for design purposes, because of rounding of member sizes, material resistance factors, differences between nominal and actual yield strengths, strain hardening, and the increased load necessary to form a global collapse mechanism (Mitchell et al. 2003). Hence, the 1990 calibration factor, U, was replaced by a more physically meaningful factor, which reflects the overstrength of different types of lateral load resisting systems.

3.11.3 Foundation Effects

In previous Codes, foundation factors did not vary with period, nor with intensity of ground motion. Finn and Wightman (2003; 2004) proposed two factors to account for these effects: an acceleration-related site coefficient, F_a, for the short-period response, and a velocity-related site coefficient, F_v, for long-period response. These are applied to the spectral acceleration ordinates to modify the design spectrum.

$$S(T) = \begin{cases} F_a S_a(0.2s) & \text{for } T \le 0.2s, \\ F_v S_a(0.5s) \text{ or } F_a S_a(0.2s) \text{, whichever is smaller,} & \text{for } T = 0.5s, \\ F_v S_a(1.0s) & \text{for } T = 1.0s, \\ F_v S_a(2.0s) & \text{for } T = 2.0s \text{, or} \end{cases} \qquad [3.23]$$

$$\frac{F_v S_a(2.0s)}{2} \qquad \text{for } T \geq 2.0s\,.$$

3.11.4 Spectral Effects

The period-dependent variation of base shear in earlier code editions (NBCC 1985, 1990, 1995) was obtained by multiplying the zonal velocity ratio, *v*, by a seismic response factor, *S*, which depended on the ratio of zonal acceleration to zonal velocity. However, the Uniform Hazard Spectra (UHS) adopted for this edition of the NBCC better capture the spectral variation of seismic hazard, as spectral acceleration ordinates are specified at different periods, thus removing the need to scale peak values.

An attempt was also made to refine the estimation of the building period. The alternate formulae for steel and reinforced concrete moment resisting frames were adopted, and new formulae were suggested for the period of steel braced frames and shear wall structures.

$$T = 0.085h^{3/4} \quad \text{for steel MRF,} \tag{3.24}$$

$$T = 0.075h^{3/4} \quad \text{for RC MRF,} \tag{3.25}$$

$$T = 0.1N \quad \text{for other MRF,} \tag{3.26}$$

$$T = 0.025h \quad \text{for steel braced frames, and} \tag{3.27}$$

$$T = 0.05h^{3/4} \quad \text{for SW and other structures.} \tag{3.28}$$

The addition of the formula for steel braced frames resulted from work by Tremblay (2005), and the other formulae were based on the recommendations of Saatcioglu and Humar (2003). As this is an important part of the proposed research, this topic will be discussed in more detail in section 4.

3.11.5 Distribution of Seismic Forces and Higher Mode Effects

As was the case in all previous editions of the Code, the ESFP was based on the assumption that the response of the structure could be adequately represented by a first mode response only, at the fundamental period of the structure. As mentioned previously, in long period structures, higher modes typically contribute considerably to the overall response. In past Codes, these higher mode effects were addressed by assigning a portion of the calculated base shear to the top storey of the structure, F_t, to augment the shears in the upper storeys; allocating the remaining base shear according to an approximately triangular distribution; and adjusting the overturning moments obtained from this load distribution by a reduction factor, *J*.

Humar and Mahgoub (2003) undertook a numerical study to examine the differences in shear distribution along the height of a structure resulting from the ESFP, as opposed to a response spectrum analysis using the UHS. Recognizing that UHS are a composite of many earthquakes, and as such can not be considered response spectra, the authors first showed that the results from response spectrum analyses using the UHS closely matched results from modal superposition analyses using appropriate simulated earthquakes (Atkinson and Beresnev 1998). They concluded that UHS could be used in response spectrum analysis without undue conservatism.

Next, they considered several types of structures: flexural wall buildings, moment frame buildings, concentrically-braced frames, coupled flexural wall systems, and hybrid frame-wall systems. A number of models were created to account for the five different types of systems, considering twenty-two different cities (with different hazard levels), and different fundamental periods. In each case, they compared the elastic base shear obtained from an SRSS combination of modal responses in the numerical models using the UHS, V_{be}, to that obtained using the ESFP in the Code, V_{bc} to obtain an estimate of the higher-mode factor, M_v. They found that higher-mode effects were more important in flexural wall buildings; that braced frames were between the MRF and flexural wall behavior; that coupled walls essentially behaved as MRF; and that hybrid systems essentially behaved as flexural walls. Also, they determined that the higher-mode factor increased with period; that its rate of increase was higher in Eastern Canada (due to the shape of the design spectrum); and that it was generally higher in Eastern Canada than Western Canada. They proposed values of the higher mode factor, M_v , which capture these variations.

Further, they performed similar analyses to determine the base overturning moment reduction factors that should be applied, given the changes in the calculation of the Code base shear. They proposed revised values of the overturning moment reduction factor (as compared to previous Codes) to be used with the new base shear formula. These results, as well as those for the higher-mode factor, were incorporated directly into the NBCC 2005.

4. <u>Fundamental period studies</u>

As we have seen, a structure's fundamental period has a very important effect on the dynamic forces to which it will be exposed during a particular ground shaking event. When the ground motion has significant energy content in the range of the structure's fundamental period, the structure's response may be significantly amplified. There is thus a need to predict this parameter as accurately as possible during the design process; that is, before the structure is actually built.

This is usually done in one of two ways: either by using empirical formulae provided by building codes; or by analytical methods, such as numerical modeling, eigenvalue analysis, or Rayleigh's method. As we have seen, since 1970 the National Building Code of Canada has provided simple empirical period formulae for different types of lateral force-resisting systems, based on building geometry. Recognizing that these formulae are far from perfect (as discussed below), most loading codes allow other methods to be used to determine the fundamental period. However, these methods require the formulation of the mass and stiffness matrices (numerical modeling and eigenvalue decomposition), or certain assumptions on the mass and force distributions, as well as on the shape of the fundamental vibration mode (Rayleigh's method). To limit the possibility of grossly inappropriate assumptions, building codes typically impose limits on the period increase obtained by such methods, as compared to the empirical formulae.

Further, the earthquake engineering community has long recognized that the distribution of seismic forces is much better captured by dynamic analysis than by any equivalent static force procedure. Therefore, most current codes allow seismic design to be performed by dynamic analysis. Again, certain limits are imposed, either on the fundamental period or on the base shear obtained by dynamic analysis, to limit the possibility of gross modeling errors.

It is evident that the calculation of seismic design loads in most building codes, and more specifically in the NBCC, hinges on empirical period formulae. A critical review of these formulae will be presented here.

4.1 Critical review of empirical period formulae

As of the 1970 edition of the NBCC, the role of the fundamental period on seismic design forces was formally recognized through the use of a period-dependent response spectrum. The fundamental period was calculated using one of the following formulae:

$$T = \frac{0.05 h_f}{\sqrt{D_f}} \quad \text{for all buildings, except} \qquad [3.9]$$

$$T = 0.1N \quad \text{for all buildings in which moment resisting frames resist 100\% of the seismic design loads,} \qquad [3.10]$$

where h_f was the height of the building in feet,
D_f was the length of the building, or the length of the lateral load resisting system (depending on the edition of the NBCC), in the direction parallel to the applied forces, in feet, and
N was the number of storeys.

As mentioned in section 3.5.3, the first formula was based on data that exhibited significant scatter, but was deemed conservative for design purposes. The second formula has been in use in building codes at least since the 1960s (Housner and Brady 1963), but it is not clear what it is based on.

Using period data from 77 steel frame and reinforced concrete buildings, Housner and Brady (1963) showed that these did not provide good estimates of the fundamental period of structures. They suggested that, for use in seismic load calculations, fundamental periods should be determined by Rayleigh's method. Nevertheless, these equations remained in the Code for many years.

Several attempts were made in the last 40 years to improve these equations by considering different materials and different types of lateral force-resisting systems separately. Of course, this was only done for the more common systems. Discussed below are the main improvements that have occurred for the different types of lateral force-resisting systems.

4.1.1 Moment-resisting frames (MRF)

The estimation of the fundamental period of all moment-resisting frames, according to the NBCC, was based on Equation 3.10 until the 1995 edition, in which two alternative formulae were included to complement it:

$$T = 0.085 h_m^{3/4} \quad \text{for steel MRF, and} \qquad [3.24]$$

$$T = 0.075 h_m^{3/4} \quad \text{for RC MRF,} \qquad [3.25]$$

where h_m was the height above ground in metres.

These formulae were originally developed (with the height in feet) by the Applied Technology Council (1978), based on Rayleigh's method. In developing them, it was assumed that the base shear varied with $T^{-2/3}$; that the lateral seismic forces varied linearly along the building height; and that deflections were controlled by drift limitations (constant inter-storey drift). This resulted in the period varying approximately with $h^{3/4}$. The coefficients were then obtained by carrying out constrained regression analyses for the different building types, using acceleration data from buildings measured during the 1971 San Fernando earthquake. In total, 17 steel frames, 14 reinforced concrete frames, and 9 reinforced concrete shear wall buildings were considered (Applied Technology Council 1978). Although an improvement on the previous formula, these equations still exhibited significant scatter, as illustrated in Figures 2 and 3 (the coefficients are different because the height is in feet). Despite this, these formulae were adopted in the NBCC 2005 based on the recommendations of Saatcioglu and Humar (2003).

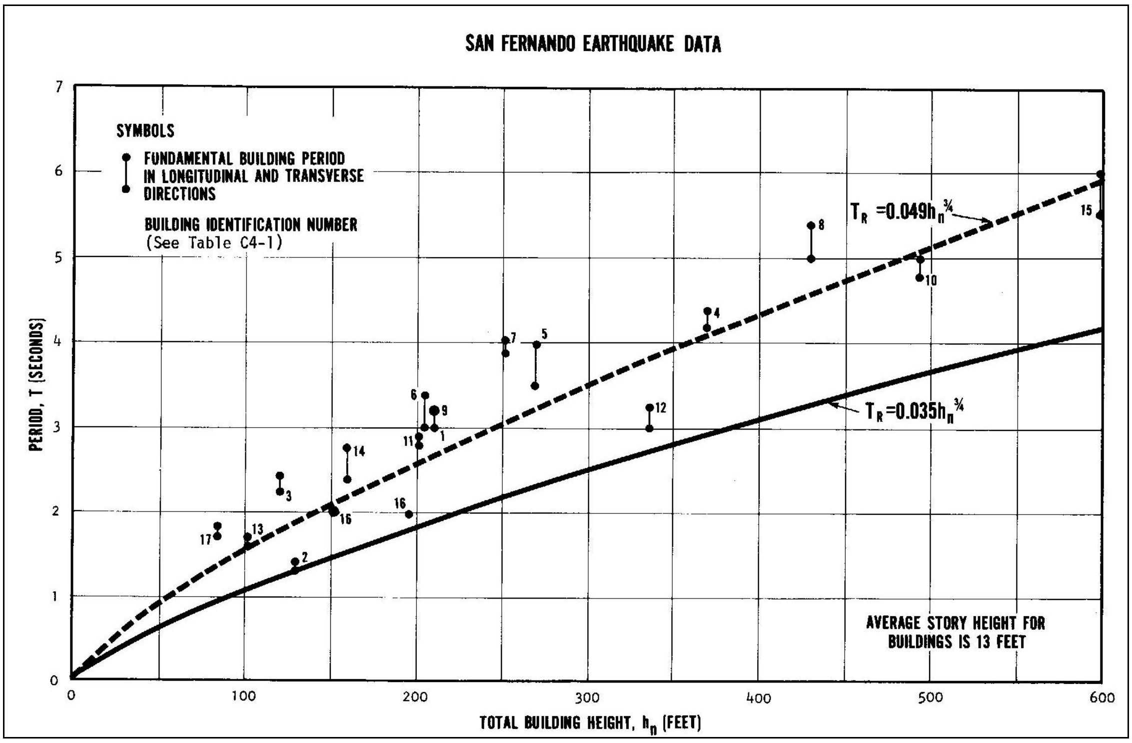

Figure 2: Period formula for steel moment frames (source: Applied Technology Council 1978)

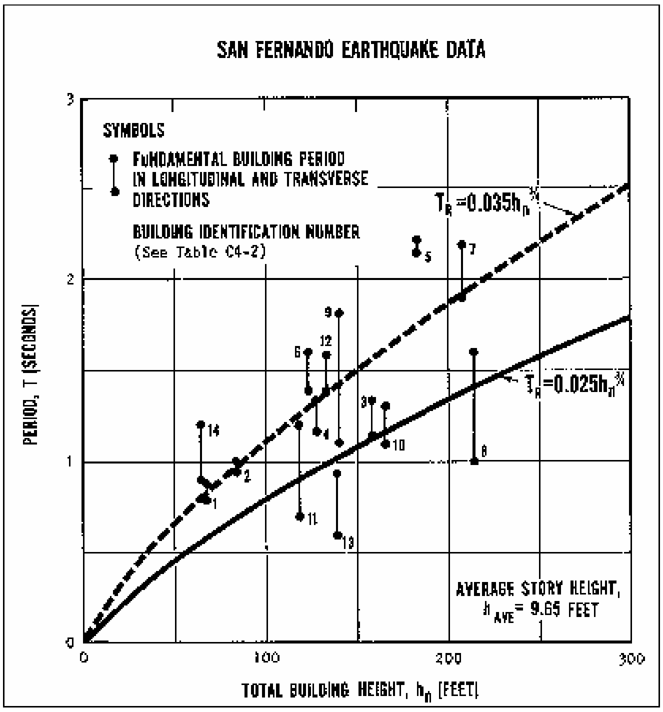

Figure 3: Period formula for RC moment frames (source: Applied Technology Council 1978)

Recognizing that these equations were based on a limited amount of data and from a single earthquake, Goel and Chopra (1997) evaluated these equations using a much larger data set, comprised of 106 buildings whose periods were measured during several California earthquakes. The buildings were classified according to their lateral structural system and 117 data points from 85 buildings were retained for analysis: 37 data points for 27 RC MRF buildings, 53 data points for 42 steel MRF buildings, and 27 data points for 16 RC shear wall buildings. Each data point consisted of two periods, one in each of the two lateral directions. Because several buildings were measured during different earthquakes, the number of data points exceeded the number of buildings (Goel and Chopra 1997). Figure 4 shows a scatter plot of fundamental periods from the expanded data set, as well as the curves corresponding to Equations 3.24 and 3.25 for steel and RC moment-resisting frames (the coefficients are different because the height is in feet).

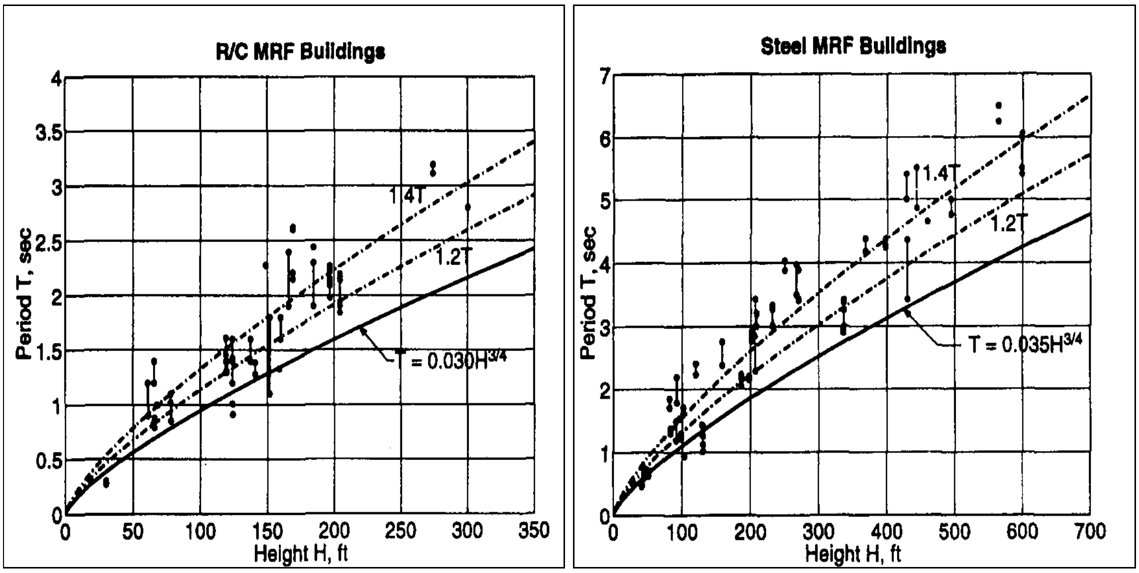

Figure 4: Comparison of measured building data and period equations for RC and steel MRF (source: Goel and Chopra 1997)

Noting that these equations fit the data rather poorly, Goel and Chopra performed regression analyses to determine whether the equations could be improved. The candidate equations were all of the form:

$$T = \alpha h_f^{\beta}, \tag{4.1}$$

where α and β were the unknown parameters to be determined from regression analysis.. As expected, the value of ¾ for the exponent β did not represent the best fit curve, and they attempted to improve the fit by increasing this value. They suggested the following formulae to determine the fundamental lateral period of MRF:

$$T = 0.016 h_f^{0.90} \quad \text{for RC MRF, and} \tag{4.2}$$

$$T = 0.028 h_f^{0.80} \quad \text{for steel MRF.} \qquad [4.3]$$

It should be noted that these improved formulae represented only a marginally better fit to the data, and that these recommendations have not been included in the National Building Code of Canada.

4.1.2 Shear wall buildings

Since few experimentally obtained periods were available for RC shear wall buildings at the time, Equation 3.9 was still suggested in the "Tentative provisions for the development of seismic regulations for buildings" (Applied Technology Council 1978) as a conservative equation to estimate the fundamental sway period of a RC shear wall building.

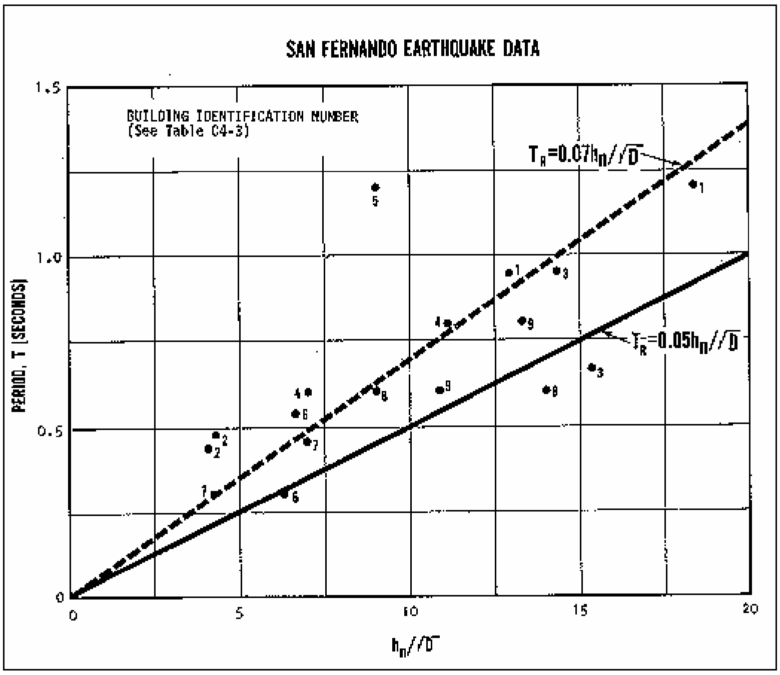

Figure 5: Period formula for shear wall buildings (source: Applied Technology Council 1978)

In fact, in Canada, this equation remained in the NBCC until the 1995 edition, inclusively (NBCC 1995a). However, there was much confusion among designers as to the estimation of the length of the lateral load resisting system, particularly in the case of multiple, coupled or perforated walls. Therefore, in the 2005 edition, the formula to determine the fundamental period of reinforced concrete shear wall buildings was changed, based on the recommendations of Saatcioglu and Humar (2003), to

$$T = 0.05 h_m^{3/4}. \qquad [3.28]$$

This equation had been in use for some time in several American codes, including NEHRP-97 (BSSC 1997).

In a companion paper to the one discussed above, Goel and Chopra (1998) evaluated the adequacy of Equation 3.28 in predicting the fundamental period of RC shear wall buildings. Relying on the appropriate buildings from the larger data set described above, they found that it was inadequate, often leading to overestimates of the fundamental lateral period of RC shear wall buildings, which is unconservative for the prediction of base shear forces. Figure 6 shows a scatter plot of the observed period data, as well as the curve representing Equation 3.28 (the coefficient differs because the height is expressed in feet).

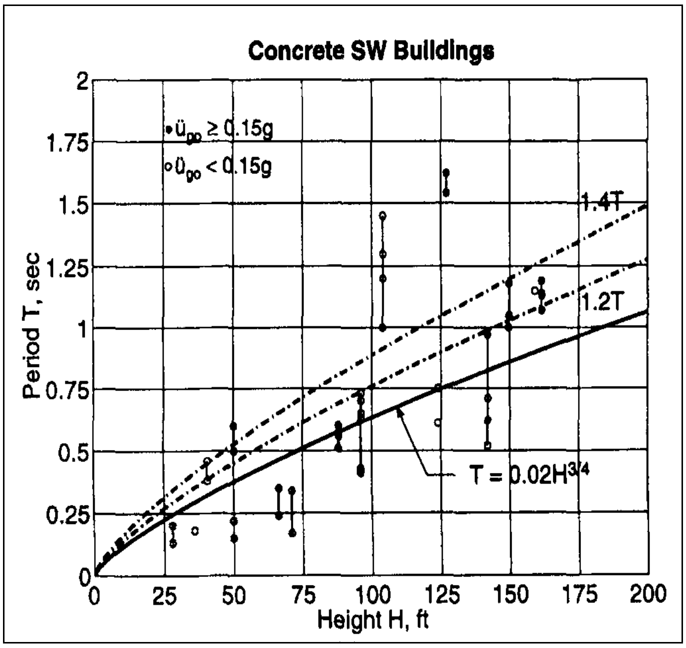

Figure 6: Period formulae for RC shear wall buildings (source: Goel and Chopra 1998)

Goel and Chopra (1998) argued that the building height alone is not sufficient to determine the fundamental sway period of an RC shear wall building. They proposed a more complex formula, based on Dunkerley's method (Jacobsen and Ayre 1958), and calibrated using regression analysis on the measured data. However, even though their new formula provided a better fit of the measured data, its increase in accuracy came at the expense of simplicity; the new formula requiring the estimation of many parameters that may be unknown at the beginning of the design process. Therefore, for simplicity, the NBCC 2005 did not adopt the suggestion of Goel and Chopra and retained a simple formula based on height alone (Equation 3.28).

4.1.3 Braced frames

Housner and Brady (1963) suggested that for most shear buildings a simple expression with the period varying linearly with building height would yield better estimates than Equation 3.9. As mentioned in the previous section, there was also much confusion about the interpretation of the length of the lateral load resisting system in this equation. Nevertheless, the change was never incorporated into the NBCC, prior to 2005. Considering this, Tremblay (2005) undertook an analytical study of different types of steel braced frames.

Tremblay first reviewed a few experimental studies where the periods of steel braced frames were reported and compared to predictions based on analytical or numerical models. He suggested that the fundamental period of steel braced frames could be accurately predicted from analytical models. He then reviewed a large database of steel braced frames reported in the literature, for which the fundamental periods were analytically computed. The database was comprised of 220 structures - 195 concentrically-braced frames (CBFs) and 25 eccentrically-braced frames (EBFs) – among which only 3 structures of each type were actual structures. The remaining structures were textbook examples or simple hypothetical structures, roughly three quarters (159) of which were designed according to the seismic provisions of the Canadian building codes (NBCC 1990a; 1995a; 2005a); and the others were designed by U.S. (42), New Zealand (10) or European (9) building codes. These data were then used to examine the validity of previous building code formulae and evaluate the influence of building geometry and seismic hazard level on the fundamental period. Tremblay then presented an extensive parametric study to establish a conservative empirical formula for braced steel frames. In this study, all structures were designed using the equivalent static procedure of the NBCC 2005 provisions and the CSA-S16 Standard for the design of steel structures in Canada, considering different cities (seismic hazard), soil conditions, building geometries, and building importance. The periods were then computed using a closed-form solution based on Rayleigh’s method. Figure 7 shows a scatter plot of the results of this study.

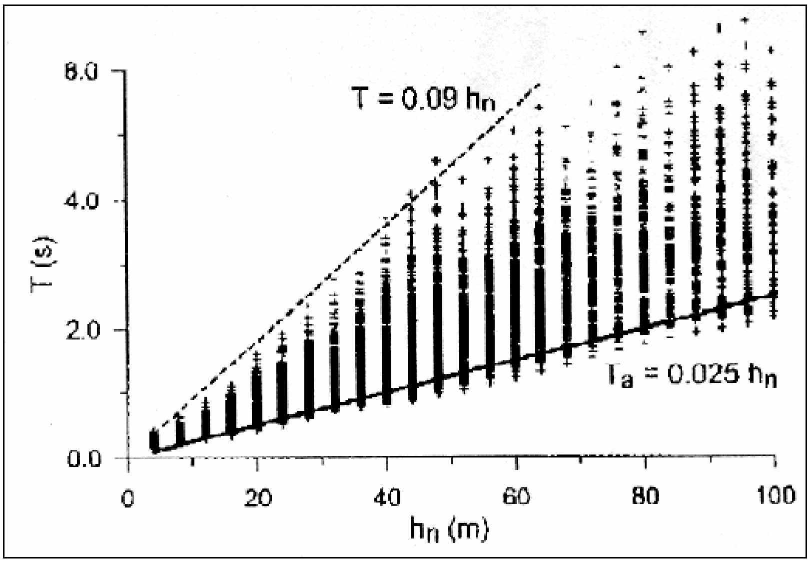

Figure 7: Braced frame period formula (source: Tremblay 2005)

This study confirmed that a linear variation of period with building height was more appropriate for steel braced frames, and that the implied precision of Equation 3.9 was not justified. Tremblay suggested the following equation as a conservative estimate of the fundamental period for all steel braced frames (both concentrically and eccentrically braced) – see Figure 7 above.

$$T = 0.025 h_m \qquad [3.27]$$

However, Tremblay cautioned that field measurements were required to validate these analytical findings, which were essentially based on "numerical" building designs. Nevertheless, Equation 3.27 was adopted by the NBCC 2005.

4.2 Period formulae in NBCC 2005

In the most recent (2005) edition of the NBCC, the fundamental period which is to be used in determining the design spectral acceleration is calculated by one of the following formulae:

$$T = 0.085 h_m^{3/4} \quad \text{for steel MRF,} \qquad [3.24]$$

$$T = 0.075 h_m^{3/4} \quad \text{for reinforced concrete MRF,} \qquad [3.25]$$

$$T = 0.1 N \quad \text{for other MRF,} \qquad [3.26]$$

$$T = 0.025 h_m \quad \text{for braced frames, and} \qquad [3.27]$$

$$T = 0.05 h_m^{3/4} \quad \text{for shear walls (SW) and other structures.} \qquad [3.28]$$

As we have seen, most of these equations represent a relatively poor fit to measured period data. Though the Code allows other methods (numerical modeling, eigenvalue analysis, or Rayleigh's method) to be used to determine the fundamental period of a structure, it also imposes restrictions on the periods thus obtained, based on the above empirical formulae. There is therefore a need to refine these formulae, as the estimation of the fundamental period of a structure plays an important role in the determination of seismic design loads.

Clearly, the goal is to have simple but rational equations, which provide reliable estimates of the fundamental period of vibration of different structures, *as they respond to their design earthquake ground motions*. As mentioned in section 1, the fundamental period of a structure tends to increase with increasing excitation amplitude. The period database on which these formulae are based was obtained from buildings in California whose periods were measured during several earthquakes; each causing ground motions of significantly different amplitudes at each location. This data set is thus somewhat inconsistent. This study aims to provide a consistent data set for the low-amplitude fundamental periods of buildings in Montreal, which could be used as an initial conservative estimate for design purposes. Better estimates of the actual period expected during the design ground motion should come from magnitude-period elongation relations, the development of which is left for future studies.

Finally, Equation 3.27 was based on an analytical study; hence there is a need to confirm its validity using experimental data.

5. Experimental Modal Analysis

In the preceding sections, it was shown that the fundamental period plays an important role in the determination of seismic design forces, and that the empirical equations provided in building codes to estimate the fundamental period rely on limited, somewhat inconsistent, data, which exhibit significant scatter. It is thus suggested to attempt to improve these formulae based on the measured dynamic properties of existing buildings. This section will discuss the different ways of obtaining the dynamic properties of a structure from measured data, with emphasis on modal parameter identification using ambient vibration data.

In section 2, it was shown that the dynamics of a structure could be expressed in a simple form by making use of its natural vibration modes – frequencies, damping ratios and mode shapes. These parameters can of course be derived analytically from the mass, stiffness, and damping matrices by solving the eigenvalue problem. However, accurately generating these matrices can be a laborious, if not impossible, task, as much for buildings in the design stage, as for built structures. On the other hand, different testing methods allow the identification of the modal parameters of a structure from vibration measurements without unreasonable effort. This identification is commonly referred to as Experimental Modal Analysis (EMA).

EMA is not only useful for seismic applications; it is used widely in the mechanical and aerospace industries, and also significant research has been undertaken to attempt to use it for structural damage evaluation (Bolton 2007) and structural health monitoring (Darbre and Proulx 2001), as well as numerical model validation and updating (Arman et al. 2007). The most common test methods, as well as their advantages and disadvantages, will be discussed below.

5.1 Input/Output Modal Analysis

Traditionally, EMA has been performed in the context of input/output modal tests to build modal models of structures. The simplest of these tests involves exciting a structure with a known input at a specific degree of freedom and measuring a single response component at a particular degree of freedom (the same or different). This is referred to as a Single-Input-Single-Output test (SISO).

Recall from Equation 2.30 that the input and output at any two DOFs can be related through an FRF. Conversely, if the input is known and the output is measured, the FRF relating the input to the output, which contains the information about the modal properties, can be estimated by computing the ratio of the output and input Fourier spectra (Maia et al. 1997).

$$H(\omega) = \frac{U(\omega)}{F(\omega)} \qquad [5.1]$$

However, FRFs are usually estimated using spectral densities, rather than Fourier spectra directly. Two common FRF estimators are denoted $H_1(\omega)$, $H_2(\omega)$.

$$H_1(\omega) = \frac{P_{fu}(\omega)}{P_{ff}(\omega)}, \text{ and} \qquad [5.2]$$

$$H_2(\omega) = \frac{P_{uu}(\omega)}{P_{uf}(\omega)}, \qquad [5.3]$$

where $P_{fu}(\omega)$ is the cross-spectral density between the input (f) and the output (u), and similarly for the other terms. Often, both estimators are used, and they are compared using the ordinary coherence function.

$$\gamma^2(\omega) = \frac{H_1(\omega)}{H_2(\omega)} \qquad [5.4]$$

Since both estimators should theoretically yield the same result, the ordinary coherence function is an indicator of the quality of the estimated FRF. A third estimator, $H_3(\omega)$, is also used when the test involves an external white noise input force, $r(t)$, in addition to the input, $f(t)$ (Maia et al. 1997).

The excitation itself can vary in character, from a harmonic excitation (which excites a particular frequency), to a transient force (e.g. from an impact hammer), to white noise (exciting all frequencies approximately equally). For example, a sine sweep SISO test can be used to identify the modal parameters of a system by slowly varying the frequency of a harmonic excitation until the response is amplified. Evidently, it is also possible to excite several DOFs with different forces, and to measure the responses at different DOFs, giving rise to Single-Input-Multiple-Output (SIMO), Multiple-Input-Single-Output (MISO) and Multiple-Input-Multiple-Output (MIMO) tests.

A number of different algorithms have been developed over the years to obtain the modal parameters of a system from input/output modal tests. In general, these are separated into those that carry out the identification in the time domain, and those that carry it out in the frequency domain. A further category, known as subspace algorithms, relies on a state-state formulation of the equations relating the inputs and the outputs. Some of the more common algorithms for input/output modal testing are the Complex Exponential (CE), Polyreference Complex Exponential (PRCE), Ibrahim Time Domain (ITD), and ARMA-based time domain methods; as well as the Peak Amplitude, Circle-Fitting Frequency Domain Complex Exponential (FDCE), and Polyreference Frequency Domain (PRFD) frequency domain methods; and finally subspace methods such as the Eigensystem Realization Algorithm (ERA) (Maia et al. 1997). This testing method and the different algorithms are well documented in several books on EMA; two of the more notable being (Ewins 2000) and (Maia et al. 1997).

The main advantage of input/output tests is that both the system response and the input forces are known. It is thus possible to obtain reliable estimates of the modal parameters using the FRF estimators. However, testing large civil engineering structures by such means can be a difficult task. Artificial excitation of large structures requires large shakers, which may cause the tests to take a considerable amount of time, and may also affect the measured properties due to mass loading effects. Also, in such structures, the ambient loads are always present in addition to the test loads, thereby compromising the input/output relationship (Parloo et al. 2003).

5.2 Free Response Tests

Free response tests involve subjecting a structure to a set of initial conditions – for example by displacing the structure into a particular deformed configuration – and measuring the response over time. Alternatively, the structure can be impacted to produce initial conditions on velocity, rather than displacement. Or, the structure can be excited at a particular frequency until the response amplitudes are large enough, and then the excitation removed and the free vibration response measured (Schiff 1972). ITD is a popular modal identification tool for free response data.

5.3 Earthquake Response Tests

Earthquake response tests consist of permanently installing sensors in the building whose modal properties are sought, waiting for relatively strong ground shaking to occur, and simultaneously measuring the ground shaking and the structure's corresponding response. For earthquake engineering purposes, these clearly represent the best testing method as they provide an estimate of the dynamic properties of the structure during an actual ground shaking event. The reason is that these properties tend to vary with the intensity of the ground shaking (McVerry 1979; Trifunac et al. 2001a; Udwadia and Trifunac 1974). However, in areas of low to moderate seismicity, these tests may be difficult to perform as it may take long before an earthquake occurs that causes significant ground shaking at the building location. Further, as mentioned above, these types of tests require the permanent instrumentation of the building under study; therefore a large number of sensors are required to obtain reliable information on the spatial variation of the response (mode shapes).

5.4 Ambient Modal Analysis (AMA)

Ambient vibration tests (or AMA), rely on low-amplitude excitation from ambient sources, such as wind and micro-tremors, to drive building motion, which is measured and analyzed to obtain the vibration properties of the structure. In this type of analysis, the input forces are not measured. Therefore, to extract the modal parameters of the system, the excitation is usually assumed to have the properties of a broadband, stationary Gaussian white noise (Brownjohn 2003). This implies that the excitation has approximately equal energy content throughout the frequency range of interest. The method is sometimes referred to as output-only modal analysis or operational modal analysis (OMA).

AMA has been widely touted as a practical modal identification technique, mainly due to its easy and inexpensive setup, as well as the fact that the modal properties are obtained under the actual operating conditions of the structure. It has been shown to yield good estimates of the natural frequencies and mode shapes under normal operating conditions, but estimates of modal damping ratios are not very reliable because the amplitudes of motion generated are typically small, hence the uncertainty on relative amplitude decays (Brownjohn 2003).

The first known report of vibration experiments using ambient vibrations was a study of the fundamental periods of structures by the U.S. Coast and Geologic Survey (Carder 1936; Ivanovic et al. 2000b). The method began to stimulate wide interest after the work of Crawford and Ward (1964), who sought to compare the experimental vibration periods of actual buildings with those predicted from mathematical models. They showed that ambient tests could be used to find the first few natural frequencies and corresponding mode shapes of a structure. Since then, a very large number of studies have been published on the subject. The following are some of the more important studies, as pertains to this particular research project, and are by no means an exhaustive list of references on the subject.

Over the years, ambient vibration tests have been conducted on a wide range of full-scale structures to obtain their modal parameters, including buildings (Beck et al. 1995; Ivanovic et al. 2000a), bridges (Brownjohn et al. 1999; Farrar and James III 1997), and dams (Darbre et al. 2000). Also, many studies compared the dynamic characteristics obtained from ambient vibration tests with those obtained from other testing methods, and investigated the effects of excitation amplitude on the measured properties. Trifunac (1972) compared the results of ambient and forced vibration tests on two buildings in California: the San Diego Gas and Electric Company building and the Robert Millikan Library. He showed that the results of ambient and forced vibration tests agreed very well, but that slight reductions in frequencies could be expected in forced vibration tests when the excitation amplitudes (between the different testing methods) were significantly different. These findings were confirmed by other authors (Hans et al. 2005). Udwadia and Trifunac (1974) compared the results of ambient, forced and earthquake tests on the Robert Millikan Library and a steel frame building at the Jet Propulsion Laboratory of the California Institute of Technology. They showed that the apparent natural frequencies during moderate ground shaking were significantly lower than those from lower amplitude excitations (ambient and forced vibration tests and smaller earthquakes), but that the buildings seemed to recover some of their lost stiffness over time. This recovery appeared to be almost immediate in the case of small ground motions, but took longer in the case of stronger ground motions. This phenomenon was later attributed mainly to soil-structure interaction (Trifunac et al. 2001a; Trifunac et al. 2001b). Other similar studies explored the changes in system parameters before and after retrofit (Celebi and Liu 1998) during construction (Memari et al. 1999), due to non-structural elements (Pan et al. 2006), and due to water level in a dam reservoir (Proulx et al. 2001).

Another important aspect of ambient vibration research is the development of algorithms to treat ambient data, often referred to as System Identification (SI). Crawford and Ward (1964) used a harmonic wave analyzer to perform a Fourier analysis of measured velocity data to obtain the power spectral density curves, which are a measure of the energy per unit frequency (Roberts and Mullis 1987). The development of the FFT algorithm (Cooley and Tukey 1965) and the advent of more powerful computers gave rise to many frequency domain SI techniques. The simplest and most common method, which is still used to some extent today, is known as the peak-picking (or basic frequency domain) method. It consists of plotting the spectral density curves and extracting the frequencies from peaks in the curves. The mode shapes are estimated by examining the relative magnitudes of the PSD curves of the different measurement channels, and the damping by the half-power bandwidth method (Craig and Kurdila 2006). In a series of papers, Akaike (1969a; 1969b) suggested first fitting an autoregressive (AR) model to the time series data to improve the spectral density estimates. AR-based SI methods began attracting increasing attention from then on (Gersch and Martinelli 1979; Gersch et al. 1973; Kadakal and Yuzugullu 1996). Many other algorithms have been introduced over the years using Hilbert-Huang transforms (Yang et al. 2003), neural networks (Huang et al. 2003), and a subspace approach (Van Overschee and De Moor 1993), many of which have not achieved widespread popularity. The most popular algorithms currently used for system identification from ambient vibration data are the Frequency Domain Decomposition (FDD) method (Brincker et al. 2001b) and the Stochastic Subspace Identification (SSI) method (Van Overschee and De Moor 1993). Both methods are quite robust, and have been used successfully by many researchers to treat ambient vibration data. However, due to its simplicity as compared to SSI, FDD will be used in this study.

Recently, most studies in the ambient vibration literature have focused on algorithm development, Finite Element model updating (Yuen and Katafygiotis 2005), structural health monitoring (Darbre and Proulx 2001), as well as damage detection (Weber et al. 2007) and localization (Duan et al. 2005).

In this study, AMA and FDD will be used to determine the modal parameters of a significant number of buildings. As mentioned previously, these will represent the low-amplitude properties of the structures (sometimes erroneously referred to as the linear properties), and it is expected that their periods will lengthen during strong ground shaking. However, since the empirical formulae to determine the fundamental frequencies of structures were derived from ground motions of different amplitudes, and that the data used to generate them exhibit such large scatter, this study will aim to provide better representation of the low-amplitude modal properties. The quantification of the amplitude-dependence of these properties will be left to future studies.

6. Ambient Vibrations: A Stochastic Process

Data obtained from ambient vibration tests are generally time histories of the displacement, velocity or acceleration response of a set of DOFs. Each of these time histories can be considered as a realization of a stochastic (or random) process. This means that future values cannot be accurately predicted and must instead be described by probabilities and statistical averages (Bendat and Piersol 2000). Thus, analysis of ambient data borrows heavily from the theory of random data analysis, the relevant aspects of which are discussed below.

6.1 Terminology and Important Statistical Properties

Suppose a stochastic process, *x(t)*. Any single observation of *x(t)* represents one of many possible results. A single time history function is therefore called a *sample record* $x_k(t)$, and represents a single *realization* of the stochastic process. A collection of sample records is called an *ensemble*.

The two most common properties used to describe stochastic processes are the mean value and the autocorrelation function, respectively defined as:

$$\mu_x = E\left[x(t)\right] \qquad [6.1]$$

$$R_{xx}(\tau) = E\left[x(t)\,x(t+\tau)\right]. \qquad [6.2]$$

6.2 Stationary and Ergodic Processes

The above properties can be estimated by averaging across an ensemble at a particular instant in time t_1.

$$\mu_x(t_1) = E\left[x(t_1)\right] = \lim_{N\to\infty} \frac{1}{N}\sum_{k=1}^{N} x_k(t_1) \qquad [6.3]$$

$$R_{xx}(t_1, t_1+\tau) = E\left[x(t_1)\,x(t_1+\tau)\right] = \lim_{N\to\infty} \frac{1}{N}\sum_{k=1}^{N} x_k(t_1)\,x_k(t_1+\tau) \qquad [6.4]$$

If the calculated mean and autocorrelation properties are the same, regardless of the instant of time selected, the process is said to be *weakly stationary*. A *strongly stationary* process has the same time invariant characteristics for all of its statistical properties (i.e. including its higher moments).

However, the statistical averages can also be estimated by averaging across time in a particular sample record, $x_k(t)$.

$$\mu_x(k) = E\left[x_k(t)\right] = \lim_{T\to\infty} \frac{1}{T}\int_0^T x_k(t)\,dt \qquad [6.5]$$

$$R_{xx}(k,\tau) = E\left[x_k(t)\,x_k(t+\tau)\right] = \lim_{T\to\infty} \frac{1}{T}\int_0^T x_k(t)\,x_k(t+\tau)\,dt \qquad [6.6]$$

An *ergodic* process is one in which the time-averaged properties are identical for all sample records, and are equal to the corresponding ensemble averages. Therefore, an ergodic process is necessarily stationary, but a stationary process is not necessarily ergodic. Since few – often only one - records are typically obtained at each location in ambient vibration tests, it is common to assume that the process is ergodic, such that the analysis can be performed using a single record for each DOF.

6.3 Spectral Density Estimation

As mentioned in section 2.5.2, the spectral density of a signal (or between two signals) is a measure of the energy content per unit frequency. The spectral density between signals *x(t)* and *y(t)* having corresponding Fourier Transforms *X(ω)* and *Y(ω)* is defined as

$$P_{xy}(\omega) = E\left[X(\omega)Y(\omega)^*\right]. \qquad [6.7]$$

An initial estimate of the spectral density can be obtained by performing an FFT for each raw time signal to obtain *X(ω)* and *Y(ω)* and simply omitting the expected value operation. However, this estimate, known as the *periodogram*, has very large variance, and fluctuates significantly about the true spectrum (Oppenheim and Schafer 1975). To improve the estimate, the approach most commonly used is to divide each data set into a series of windows of shorter duration. For each window, the periodogram is calculated. An improved estimate of the spectral density is then obtained by averaging across the different windows.

$$P_{xy}(\omega) = \frac{1}{k}\sum_{m=1}^{k} X^m(\omega)Y^m(\omega)^* \qquad [6.8]$$

In the above equation, *k* represents the number of windows and *m* is an index referring to a particular window (not an exponent). In this case, the two time history records *x(t)* and *y(t)* would need to have been divided into the same number of windows. This method of averaging periodograms, commonly referred to as Bartlett's method, significantly reduces the variance of the spectral density estimates (Oppenheim and Schafer 1975). The procedure is illustrated in Figure 8.

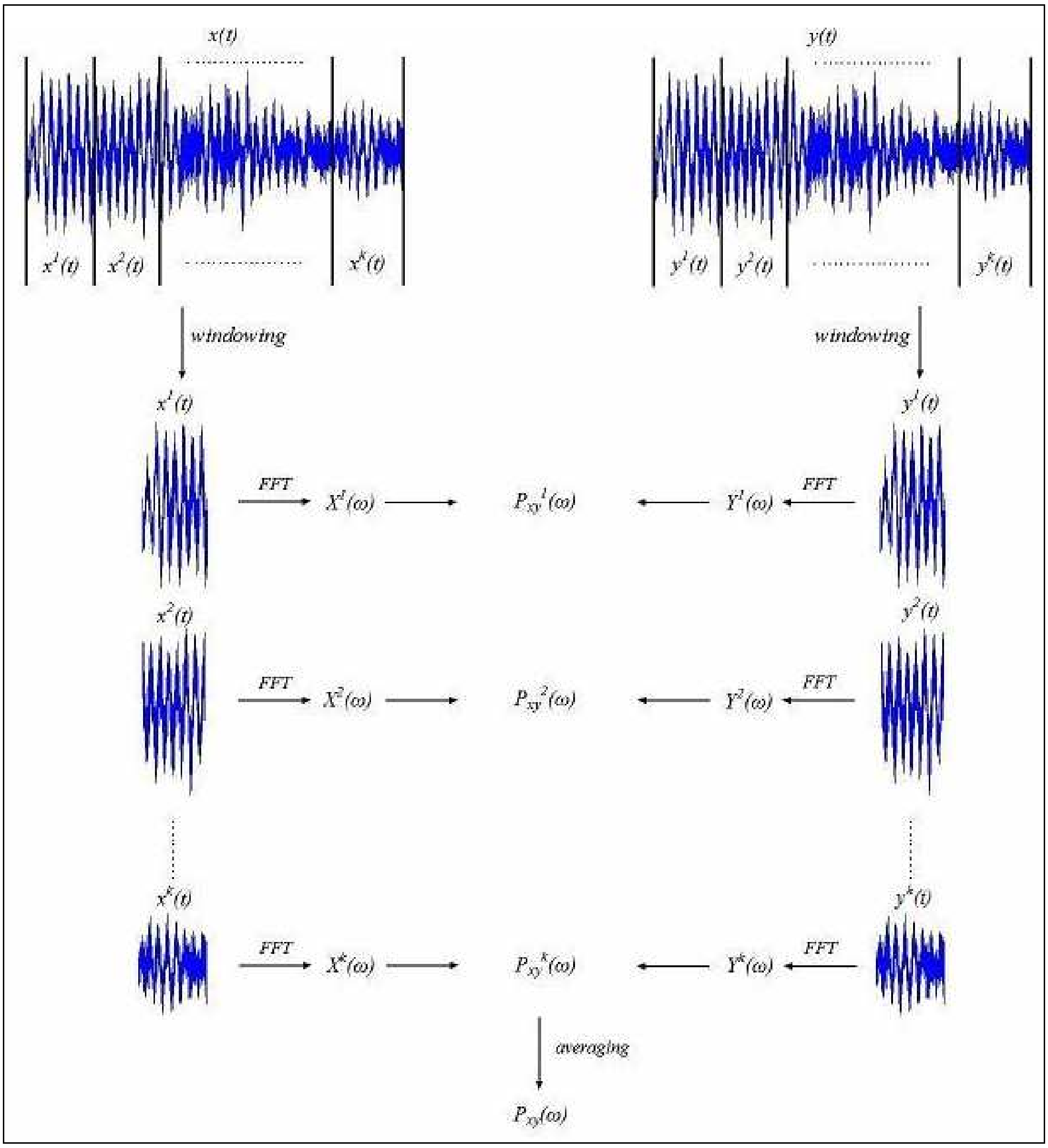

Figure 8: Illustration of Bartlett's method

However, Bartlett's method is still prone to error due to a phenomenon known as *leakage*, whereby power from a particular frequency *leaks* to neighboring frequencies due to the FFT operation. To circumvent this problem, each window is first multiplied by a leakage reduction window and then the FFT operation is performed. This method is known as the modified periodogram approach (or Welch's method) and the most common leakage reduction window is the Hanning window (Bendat and Piersol 2000). This is currently the most common way of generating spectral density functions in signal processing practice.

Alternatively, the spectral density can be estimated by Fourier transforming the correlation function. In fact, the Weiner-Khintchine relations state that the auto- (or cross-) spectral density and auto- (or cross-) correlation functions are Fourier pairs (Bendat and Piersol 2000). The continuous form of these relations is

$$P_{xy}(\omega) = \int_{-\infty}^{\infty} R_{xy}(\tau) e^{-i\omega\tau} \, d\tau, \qquad [6.9]$$

$$R_{xy}(\tau) = \frac{1}{2\pi} \int_{-\infty}^{\infty} P_{xy}(\omega) e^{i\omega\tau} \, d\omega. \qquad [6.10]$$

However, this method of spectral density estimation is not commonly used. In fact, it seems more common to use the spectral density estimated by the previous method to estimate the correlation function by Equation 6.10 (Bendat and Piersol 2000). The Weiner-Khintchine relations will be important to understanding the method used to improve frequency estimates and obtain estimates of modal damping in Frequency Domain Decomposition (section 7.2).

7. <u>Data Treatment</u>

In light of the discussion above, two data treatment procedures will be discussed: the peak-picking method and the Frequency Domain Decomposition method (FDD). The peak-picking method gained popularity mainly due its incredible simplicity and was the most widely used frequency domain method until quite recently; FDD is an extension of the peak-picking method introduced in the late 1990s, which addresses some of its shortcomings, while maintaining its simplicity.

For the following discussion, suppose ambient vibrations measurements were taken at N DOFs, giving rise to a set of time history records $x_i(t),\ i = 1, 2, \ldots, N$. For simplicity, these are shown as a set of collinear DOFs in Figure 9.

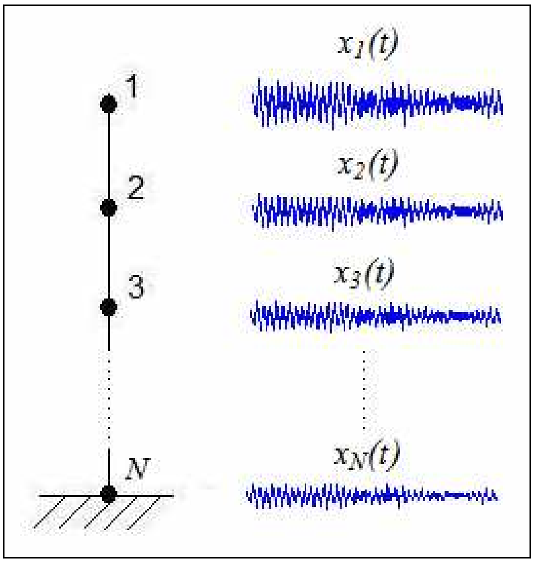

Figure 9: Example of time history records collected at N collinear DOFs

7.1 Peak-Picking Method

The peak-picking method, sometimes referred to as the Basic Frequency Domain method, essentially consists of estimating the spectral density functions between all the different signal channels (records). As mentioned in section 6.3, to obtain good estimates of the spectral density functions, it is necessary to first divide each of the N records $x_i(t)$ into k sub-records $x_i^m(t)$, $m = 1,2,\ldots,k$. These sub-records may or may not overlap. Each sub-record is then multiplied by a Hanning window to reduce the effects of leakage, generating a set of modified sub-records $y_i^m(t)$.

Then, an FFT is performed for each modified sub-record $y_i^m(t)$, thus yielding $Y_i^m(\omega)$. The power spectral density (PSD) matrix can then be computed at each frequency, for each window m, by multiplying the appropriate Fourier coefficients. For example, the entry in row j and column k, representing the spectral density between channels j and k for window m and frequency ω is

$$P_{jk}^m(\omega) = Y_j^m(\omega)Y_k^m(\omega)^*. \qquad [7.1]$$

Each element of the PSD matrix is then obtained at each frequency by averaging across all windows.

$$P_{jk}(\omega) = \frac{1}{n}\sum_{m=1}^{k} P_{jk}^m(\omega) \qquad [7.2]$$

Figure 10 illustrates the concept of PSD matrices at discrete frequencies for a 6-DOF system. The color within each cell (representing a matrix element) is used as an indicator of the magnitude of the spectral density between the channels corresponding to the cell's row and column.

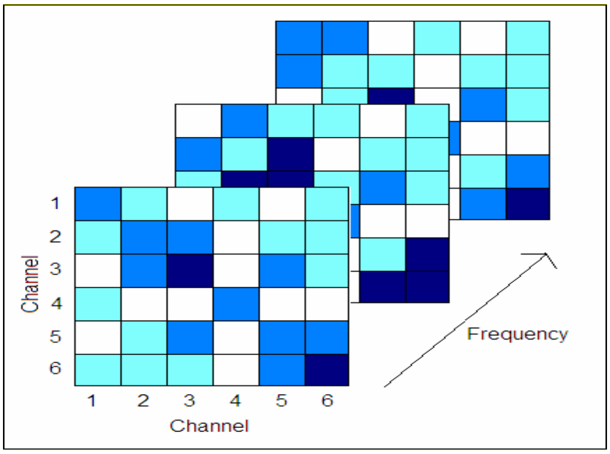

Figure 10: Illustration of PSD matrices at discrete frequencies for a 6-DOF system

Each spectral density function can then be plotted against frequency by considering one element of the PSD matrix over the entire frequency range of interest. The peaks are identified as resonance frequencies. The mode shapes can then be inferred by examining the relative magnitudes of the spectral densities of the different channels, contained in the PSD matrix at each identified resonance frequency. Modal damping ratios can be estimated by the half-power bandwidth method (Craig and Kurdila 2006) on any of the spectral density plots, but as mentioned previously these are prone to significant error.

The peak-picking technique has been shown to yield adequate estimates of frequencies and mode shapes, however it is difficult to identify closely-spaced modes (Brincker et al. 2001b). For this reason, an extension of the method, called Frequency Domain Decomposition, has gained widespread popularity in the field of ambient vibration signal processing.

7.2 Frequency Domain Decomposition

Rather than plotting the spectral densities directly, Singular Value Decomposition (SVD) of the PSD matrices is first performed. The SVD of a square matrix transforms it into a set of 3 matrices of the same size in the following way:

$$[P] = [U] \cdot [S] \cdot [V]^H , \qquad [7.3]$$

where $[P]$ is the matrix to be decomposed (in this case, the output PSD matrix at each frequency), $[S]$ is the diagonal singular value matrix, $[U]$ and $[V]$ are unitary matrices containing the orthonormal left- and right- singular vectors, respectively, and ^{H} denotes the Hermitian transformation (complex conjugate transpose). The singular values are listed in descending order along the main diagonal of [*S*] and are always real, non-negative quantities. On the other hand, the singular vectors are generally comprised of complex quantities.

If [*P*] is a Hermitian matrix, as is the case for the PSD matrix, the SVD degenerates into the spectral decomposition, hence the matrices [*U*] and [*V*] are identical.

$$[P] = [U]\cdot[S]\cdot[U]^H = \left[\{u_1\}\,\{u_2\}\cdots\{u_N\}\right]\cdot\begin{bmatrix} s_1 & 0 & \cdots & 0 \\ 0 & s_2 & \cdots & 0 \\ \vdots & \vdots & \ddots & \vdots \\ 0 & 0 & \cdots & s_N \end{bmatrix}\cdot\begin{bmatrix} \{u_1\}^H \\ \{u_2\}^H \\ \vdots \\ \{u_N\}^H \end{bmatrix} \qquad [7.4]$$

More interesting still, the singular vectors then are the orthonormal eigenvectors of [*P*], and the singular values are the corresponding eigenvalues (Schott 2005). Hence, the singular vectors represent an estimate of the directions of principal energy of the system, or the mode shapes, and the corresponding singular values provide an estimate of the contribution of each mode to the overall energy at each frequency. In other words, the SVD of the output PSD matrix is an approximation to its modal decomposition. The SVD of the PSD matrices thus allows the response spectra to be separated into a set of SDOF systems, each corresponding to a particular mode of vibration (Brincker et al. 2001b).

The SVD is carried out for each PSD matrix – i.e. at each discrete frequency resulting from the FFT operation. In practice, the first few singular values are plotted against frequency. Figure 11 shows a singular value plot obtained from the velocity time histories of a 6-DOF numerical model. The solid blue (upper) and dashed green (lower) lines represent the first and second singular values, respectively. Six resonant frequencies can be identified from the peaks in the first singular value. The first two, at frequencies of 0.61 and 0.98 Hz, represent the fundamental frequencies in each lateral direction. They are very well defined as they represent a large portion of the system's vibrational energy, but it is possible to estimate higher mode frequencies as well. Also, studying the second singular value helps identify closely-spaced modes (Brincker, et al. 2001b). When closely-spaced modes are present, the second singular value typically does not peak near the lowest frequency peak in the first singular value, as is the case for the first resonant frequency; and the next peak in the first singular value seems like a continuation of the second singular value line. Thus the first two resonant frequencies are considered closely-spaced modes. At each resonant frequency, f_p, the approximate mode shape is contained in the first singular vector $\{u_1(f_p)\}$.

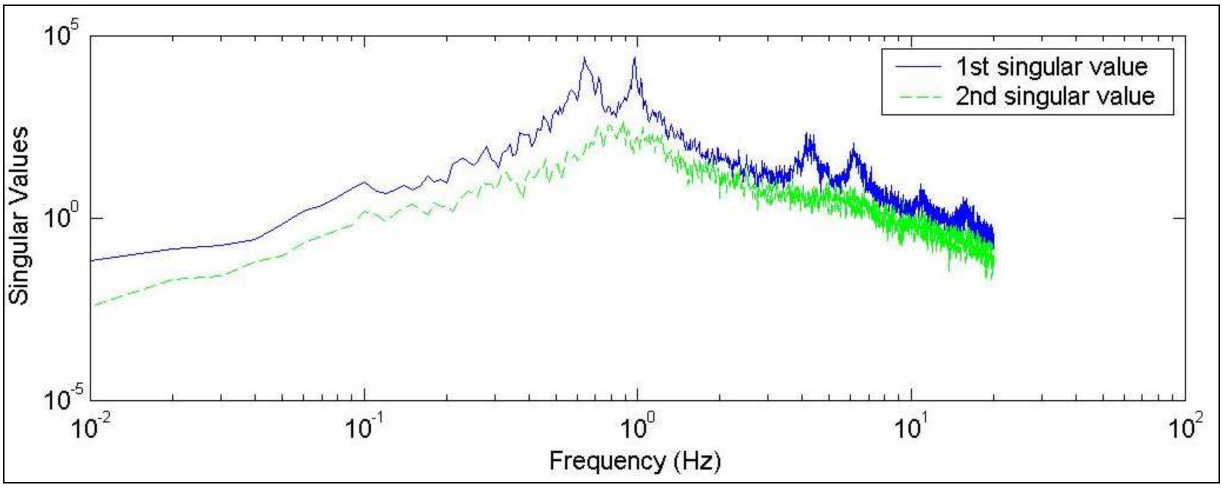

Figure 11: Typical plot of first two singular values

The method can be improved to provide better estimates of the modal frequencies and mode shapes, and also to estimate the modal damping ratios. The Modal Assurance Criterion (MAC) is introduced, which is a measure of the correlation between singular vector u_i at frequency f_1 and singular vector u_j at frequency f_2.

$$MAC\left(\{u_i(f_1)\},\{u_j(f_2)\}\right) = \frac{\left|\{u_i(f_1)\}^H \cdot \{u_j(f_2)\}\right|^2}{\left|\{u_i(f_1)\}^H \{u_i(f_1)\}\right| \cdot \left|\{u_j(f_2)\}^H \{u_j(f_2)\}\right|} \quad [7.5]$$

At a resonance frequency, f_p, the first singular vector, $\{u_1(f_p)\}$, is compared to the singular vectors at neighboring frequencies, $\{u_j(f_b)\}$, using the MAC. The idea is that a particular mode will still play an important role in the response at frequencies near to its natural frequency, thus it should still be fairly well estimated by a singular vector over a range of frequencies on either side of its natural frequency. An SDOF bell function is created by considering all the frequencies around a resonance peak that have a singular vector that has a MAC value greater than a user-defined criterion, Ω (usually around 0.8). The corresponding frequencies are denoted f_b. The SDOF bell is comprised of the singular values s_j corresponding to the singular vectors u_j, which satisfy

$$MAC\left(\{u_j(f_b)\},\{u_1(f_p)\}\right) \geq \Omega \quad [7.6]$$

In the case of well-separated modes, the singular vectors at neighboring frequencies that correlate well with the first singular vector at the resonance frequency, $\{u_1(f_p)\}$, will generally be the first singular vectors, $\{u_1(f_b)\}$. However, when closely-spaced modes are present, it is possible that higher singular vectors ($\{u_2(f_b)\}, \{u_3(f_b)\}$, etc.) will need to be considered. The resulting SDOF bell function is only defined at frequencies near the resonance frequency; the rest of the SDOF bell function – for frequencies where no singular vectors have a MAC value greater than the specified criterion – is padded with zeros (Brincker et al. 2001a). Figure 12 shows a graphical representation of the SDOF bell function. The first graph, on a log-log scale, represents a singular value plot for a 3-DOF system with well-separated modes. The portion of the first singular value (dashed blue upper line) which is highlighted in solid red – i.e. the portion around the first peak – represents the SDOF bell function. The second graph, on a semi-log scale, shows the SDOF bell function padded with zeros for frequencies where no singular vector correlates well enough with the first singular vector at the peak.

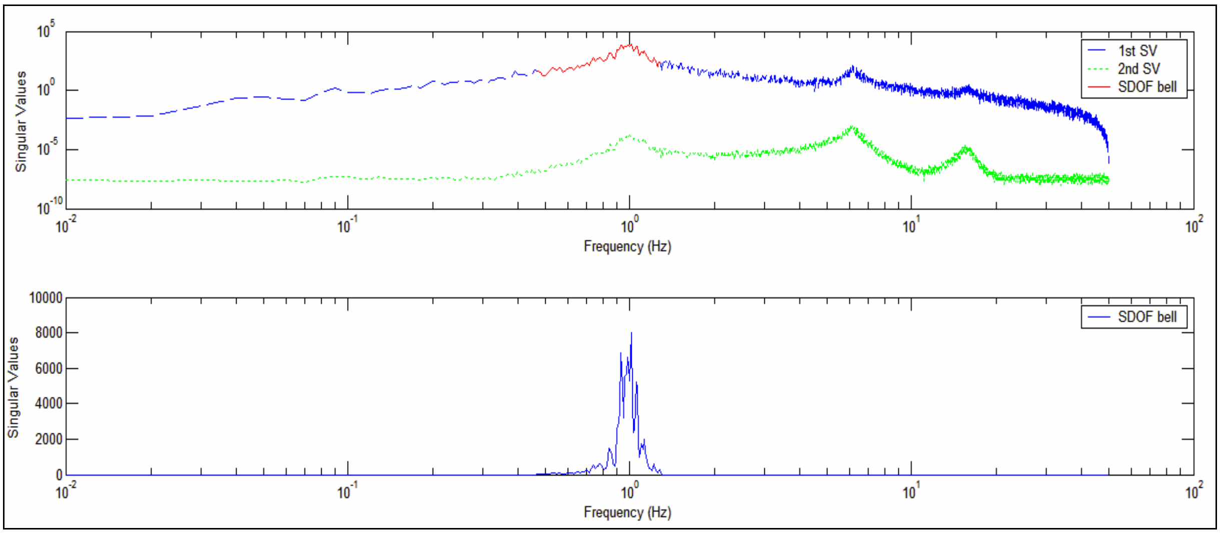

Figure 12: Graphical representation of SDOF bell function

The SDOF bell function is then brought back to the time domain (or time lag-domain) using the Inverse Fast Fourier Transform (IFFT). As mentioned in section 6.3, the Wiener-Khintchine relation states that the auto-spectral density and autocorrelation functions are Fourier pairs. Thus, the time domain function obtained from the IFFT operation is an approximation of the SDOF autocorrelation function of the corresponding mode (Brincker et al. 2001b), which decays exponentially. In general, the function thus obtained will be complex. Figure 13 shows the corresponding plot of the real (solid blue) and imaginary (dashed green) parts of the approximate SDOF autocorrelation function. It is clear that they both behave identically, only with a phase difference.

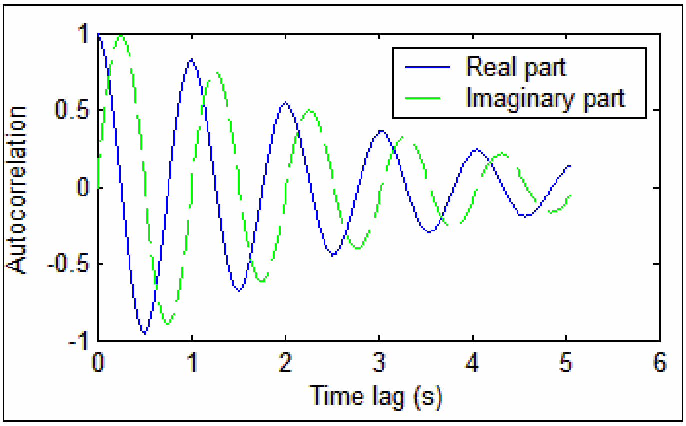

Figure 13: Approximate SDOF autocorrelation function

An improved estimate of the frequency can be obtained by counting the zero crossings of the SDOF autocorrelation function (either the real or imaginary part) (Brincker et al. 2001a). The zero crossings are plotted against time, as in Figure 14. A linear regression is then performed. Since the function crosses zero twice for each cycle, then the slope obtained from the regression – which represents the number of zero crossings per second or twice the number of cycles per second – is twice the frequency.

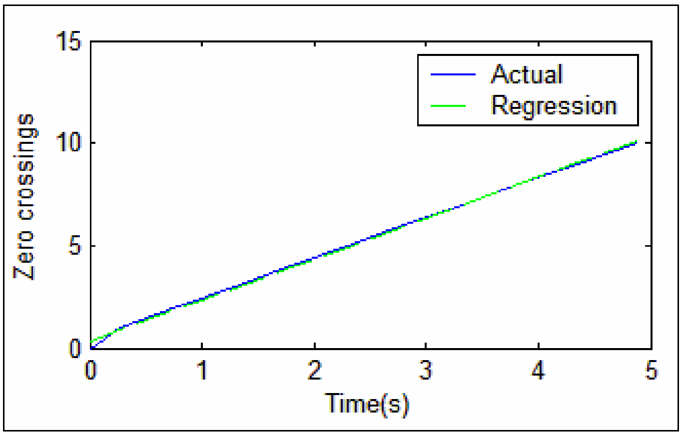

Figure 14: Linear regression on crossing times

An improved estimate of the mode shape is obtained by weighting the singular vectors from all frequencies included in the SDOF bell function by their corresponding singular values, thus giving more weight to the singular values near the peak, while still performing an averaging operation over all relevant singular vectors. The mode shape vector is normalized to unit magnitude.

$$\{\phi_p\} = \frac{\sum_{j=1}^{nbell} s_j \{u_j\}}{\left\| \sum_{j=1}^{nbell} s_j \{u_j\} \right\|}, \qquad [7.7]$$

where *nbell* is the number of singular values included in the SDOF bell function – or the number of singular vectors with a MAC value higher than Ω .

Finally, an estimate of the modal damping ratio can be obtained by the logarithmic decrement technique. The k first peaks in the autocorrelation function are identified, as well as their corresponding value, R_k. The natural logarithms of the R_k values are then plotted against the peak number, k, as in Figure 15. Again, a linear regression is performed, the slope of which yields the logarithmic decrement, Δ.

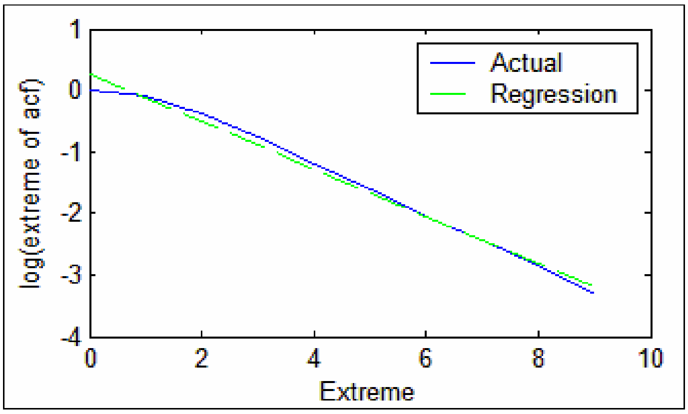

Figure 15: Linear regression to find the logarithmic decrement

And the modal damping ratio is calculated from the logarithmic decrement using (Brincker et al. 2001a)

$$\xi_r = \frac{\Delta}{\sqrt{\Delta^2 + 4\pi^2}}. \qquad [7.8]$$

In the ongoing research project, FDD is the primary method that will be used to treat the data from ambient tests. For the purposes of this study, only the fundamental sway modes in each lateral direction need to be identified. However, it will most likely be possible to identify higher modes as well. It is also hoped that estimates of modal damping ratios will be obtained; however, as mentioned previously, these are typically not very accurate.

8. Conclusion

In this report, a literature review of topics relating to the evaluation of the period formulae in the National Building Code of Canada (NBCC) using ambient vibration data was presented. First, an introduction to certain fundamental structural dynamics concepts that form the basis of all seismic design guidelines was presented. To better appreciate the importance of the fundamental period in earthquake engineering, particularly in seismic force estimation, the seismic design provisions of the NBCC and their evolution since the first edition in 1941 were then discussed. The NBCC empirical fundamental period formulae used for seismic load calculations were then reviewed. It was shown that the current equations are based on limited data from several earthquakes in California, each causing ground motions of significantly different magnitudes at each building location, thus representing a somewhat inconsistent data set. The data are quite scattered, partly because of this inconsistency, and partly because the simple empirical equations necessarily omit certain parameters that influence the fundamental periods of buildings. As a result, the equations fit the measured data rather poorly. Finally, local factors such as design and construction practices, geology, and seismicity may have an effect on the apparent fundamental periods of buildings. It was thus suggested that there is a need to evaluate, and possibly improve, the empirical period formulae for the design of structures in Montreal.

The author and his supervisor, Prof. Ghyslaine McClure, are currently undertaking a research project aimed at evaluating and improving these equations using ambient vibration data. Therefore, a review of certain key ambient vibration studies was presented here. As mentioned previously, the natural periods of a structure tend to lengthen with the amplitude of the excitation. Thus, the natural periods of a building obtained from ambient vibration tests (which represent low excitation conditions) generally underestimate the natural periods expected during strong ground motions. Some may argue therefore that ambient vibration data does not represent the likely behavior of a building during seismic ground motions. However, since seismic design loads (in the NBCC) typically decrease with increasing fundamental period, the NBCC formulae also aim to underestimate the fundamental period. There is thus a tradeoff between the conservatism of the empirical formulae and the suitability of the data on which these are based. On the one hand, data from significant ground motions better represent the likely behavior of buildings during an earthquake; but to be conservative, the equations derived from these data need to be "lower-bound" equations which may considerably underestimate the fundamental period since the data exhibit such variability. On the other hand, ambient vibration data do not represent the likely behavior as well; but the empirical equations derived from these data do not necessarily need to be "lower bound" equations since the period is expected to elongate during strong ground motions. It was suggested above that the variability in the data is a result of inconsistency in the data and the omission of certain parameters of importance in the empirical equations. It can thus be argued that using ambient vibration data could considerably reduce the data inconsistency, while still underestimating the fundamental periods of buildings. The approach proposed in this research is first to develop relations for the low-amplitude fundamental periods, and then develop relations between the excitation magnitude and the period elongation. The latter is left for future studies.

Finally, the stochastic nature of ambient vibrations and two methods of treating ambient vibration data, the peak-picking method and the Frequency Domain Decomposition method

(FDD) were also discussed. In the ongoing research project, FDD will be the main modal identification method.

9. References

Adams, J., and Atkinson, G. (2003). "Development of seismic hazard maps for the proposed 2005 edition of the National Building Code of Canada." *Canadian Journal of Civil Engineering*, 30, 255-271.

Akaike, H. (1969a). "Fitting autoregressive models for prediction." *Annals of the Institute of Statistical Mathematics*, 21, 243-247.

Akaike, H. (1969b). "Power spectrum estimation through autoregressive model fitting." *Annals of the Institute of Statistical Mathematics*, 21, 407-419.

Anderson, A. W., Blume, J. A., Degenkolb, H. J., Hammill, H. B., Knapik, E. M., Marchand, H. L., Powers, H. C., Rinne, J. E., Sedgwick, G. A., and Sjoberg, H. O. (1952). "Lateral forces of earthquake and wind." *Transactions of the American Society of Civil Engineers*, 117, 716-780.

Applied Technology Council. (1978). "Tentative provisions for the development of seismic regulations for buildings." Applied Technology Council, Palo Alto, California.

Arman, E. O., Reynders, E., Degrauwe, D., De Roeck, G., and Van den Broeck, P. (2007). "Experimental vibration analysis and finite element model updating of large structures." 2nd IOMAC, Copenhagen, Denmark.

Atkinson, G. M., and Beresnev, I. A. (1998). "Compatible ground-motion time histories for new national seismic hazard maps." *Canadian Journal of Civil Engineering*, 25(2), 305-318.

Beck, J. L., May, B. S., Polidori, D. C., and Vanik, M. W. (1995). "Ambient vibration surveys of three steel-frame buildings strongly shaken by the 1994 Northridge earthquake." California Institute of Technology, Report No. EERL 95-06, Pasadena, California.

Bendat, J. S., and Piersol, A. G. (2000). *Random data: Analysis and measurement procedures*, John Wiley & Sons, Inc., New York, N.Y., U.S.A.

Bolton, R. "A review of identification and damage assessment methods using experimental response data from the Z24 bridge." *2nd IOMAC* Copenhagen, Denmark.

Brincker, R., Ventura, C. E., and Andersen, P. "Damping estimation by frequency domain decomposition." *International Modal Analysis Conference - IMAC XIX*, Kissimmee, FL, 698-703.

Brincker, R., Zhang, L., and Anderson, P. (2001b). "Modal identification of output-only systems using frequency domain decomposition." *Smart Materials and Structures*, 10, 441-445.

Brownjohn, J. M. W. (2003). "Ambient vibration studies for system identification of tall buildings " *Earthquake Engineering and Structural Dynamics*, 32, 71-95.

Brownjohn, J. M. W., Lee, J., and Cheong, B. (1999). "Dynamic performance of a curved cable-stayed bridge." *Engineering Structures*, 21, 1015-1027.

BSSC. (1997). "NEHRP Recommended provisions for seismic regulations for new buildings and other structures - Part 1 - Provisions (FEMA 302)." FEMA, Washington, D.C.

Bustamante, J. I. "Seismic shears and overturning moments in buildings." *3rd World Conference on Earthquake Engineering*, New Zealand.

Carder, D. S. (1936). "Vibration observations, Chapter 5 in Earthquake investigations in California 1934-1935." U.S. Dept. of Commerce, Coast and Geologic Survey, Special Publication No. 201, Washington, D.C.

Celebi, M., and Liu, H.-P. (1998). "Before and after retrofit - Response of a building during ambient and strong motions." *Journal of Wind Engineering and Industrial Aerodynamics*, 77, 259-268.

Chopra, A. K. (2001). *Dynamics of structures: Theory and applications to earthquake engineering* Prentice Hall, Upper Saddle River, NJ

Clough, R. W., and Penzien, J. (2003). *Dynamics of structures*, Computers and Structures, Inc., Berkeley, CA.

Cooley, J. W., and Tukey, J. W. (1965). "An algorithm for the machine calculation of complex Fourier series." *Mathematics of computation*, 19(90), 297-301.

Cornell, C. (1968). "Engineering seismic risk analysis." *Bull. Seism. Soc. Am.*, 58, 1583-1606.

Craig, R. R., and Kurdila, A. J. (2006). *Fundamentals of Structural Dynamics*, John Wiley & Sons, Hoboken, New Jersey, U.S.A.

Crawford, R., and Ward, H. S. (1964). "Determination of the natural periods of buildings." *Bulletin of the Seismological Society of America*, 54(6), 1743-1756.

Darbre, G. R., De Smet, C. A. M., and Kraemer, C. (2000). "Natural frequencies measured from ambient vibration response of the arch dam of Mauvoisin." *Earthquake Engineering & Structural Dynamics*, 29, 577-586.

Darbre, G. R., and Proulx, J. (2001). "Continuous ambient-vibration monitoring of the arch dam of Mauvoisin." *Earthquake Engineering and Structural Dynamics*, 31, 475-480.

Duan, Z., Yan, G., Ou, J., and Spencer, B. F. (2005). "Damage localization in ambient vibration by constructing proportional flexibility matrix." *Journal of Sound and Vibration*, 284, 455-466.

Ewins, D. J. (2000). *Modal testing: Theory, practice and application*, Research Studies Press.

Farrar, C. R., and James III, G. H. (1997). "System identification from ambient vibration measurements on a bridge." *Journal of Sound and Vibration*, 205(1), 1-18.

Finn, W. D. L., and Wightman, A. (2003). "Ground motion amplification factors for the proposed 2005 edition of the National Building Code of Canada." *Canadian Journal of Civil Engineering*, 30(2), 272-278.

Finn, W. D. L., and Wightman, A. (2004). "Erratum: Ground motion amplification factors for the proposed 2005 edition of the National Building Code of Canada Ref: Can. J. Civ. Eng. 30: 272-278 (2003)." *Canadian Journal of Civil Engineering*, 31(4), 718.

Gersch, W., and Martinelli, F. (1979). "Estimation of structural system parameters from stationary and non-stationary ambient vibrations: An exploratory-confirmatory analysis." *Journal of Sound and Vibration*, 65(3), 303-318.

Gersch, W., Nielsen, N. N., and Akaike, H. (1973). "Maximum likelihood estimation of structural parameters from random vibration data." *Journal of Sound and Vibration*, 31(3), 295-308.

Goel, R. K., and Chopra, A. K. (1997). "Period formulas for moment-resisting frame buildings." *Journal of Structural Engineering*, 123(11), 1454-1461.

Goel, R. K., and Chopra, A. K. (1998). "Period formulas for concrete shear wall buildings." *Journal of Structural Engineering*, 124(4), 426-433.

Hans, S., Boutin, C., Ibraim, E., and Rousillon, P. (2005). "In situ experiments and seismic analysis of existing buildings. Part I: Experimental investigations." *Earthquake Engineering and Structural Dynamics*, 34, 1513-1529.
Hasegawa, H. S., Basham, P. W., and Berry, M. J. (1981). "Attenuation relations for strong seismic ground motion of Canada." *Bull. Seism. Soc. Am.*, 71(6), 1943-1962.
Heidebrecht, A. C. (1995). "Insights and challenges associated with determining seismic design forces in a loading code." *Bulletin of the New Zealand National Society for Earthquake Engineering*, 28(3), 224-246.
Heidebrecht, A. C., Basham, P. W., Rainer, J. H., and Berry, M. J. (1983). "Engineering applications of new probabilistic seismic ground-motion maps of Canada." *Can. J. Civ. Eng.*, 10, 670-680.
Housner, G. W., and Brady, A. G. (1963). "Natural periods of vibration of buildings." *Journal of Engineering Mechanics*, 89(EM4), 31-65.
Huang, C. S., Hung, S. L., Wen, C. M., and Tu, T. T. (2003). "A neural network approach for structural identification and diagnosis of a building from seismic response data." *Earthquake Engineering and Structural Dynamics*, 32, 187-206.
Humar, J. (2002). *Dynamics of structures*, A. A. Balkema Publishers, Exton, PA.
Humar, J., and Mahgoub, M. A. (2003). "Determination of seismic design forces by equivalent static load method." *Canadian Journal of Civil Engineering*, 30, 287-307.
Ivanovic, S. S., Trifunac, M. D., Novikova, E. I., Gladkov, A. A., and Todorovska, M. I. (2000a). "Ambient vibration tests of a seven-story reinforced concrete building in Van Nuys, California, damaged by the 1994 Northridge earthquake." *Soil Dynamics and Earthquake Engineering*, 19(6), 391-411.
Ivanovic, S. S., Trifunac, M. D., and Todorovska, M. I. (2000b). "Ambient vibration tests of structures - A review." *ISET Journal of Earthquake Technology*, 37(4), 165-197.
Jacobsen, L. S., and Ayre, R. S. (1958). *Engineering vibrations*, McGraw Hill, Inc., New York, N. Y.
Kadakal, U., and Yuzugullu, O. (1996). "A comparative study on the identification methods for the autoregressive modelling from the ambient vibration records." *Soil Dynamics and Earthquake Engineering*, 15, 45-49.
Maia, N. M. M., Silva, J. M. M. e., He, J., Lieven, N. A. J., Lin, R. M., Skingle, G. W., To, W.-M., and Urgueira, A. P. V. (1997). *Theoretical and experimental modal analysis*, Research Studies Press, Baldock, England.
McGuire, R. (1976). "FORTRAN computer program for seismic risk analysis." *Open-file Report 76-67*, U.S. Geological Survey.
McVerry, G. H. (1979). "Frequency domain identification of structural models from earthquake records," California Institute of Technology, Pasadena, California.
Memari, A. M., Aghakouchak, A. A., Ashtiany, M. G., and Tiv, M. (1999). "Full-scale dynamic testing of a steel frame building during construction."
Mitchell, D., Tremblay, R., Karacabeyli, E., Paultre, P., Saatcioglu, M., and Anderson, D. L. (2003). "Seismic force modification factors for the proposed 2005 edition of the National Building Code of Canada." *Canadian Journal of Civil Engineering*, 30, 308-327.
NBCC. (1941). "National Building Code of Canada 1941." National Research Council of Canada, Ottawa, Ontario.
NBCC. (1953). "National Building Code of Canada 1953." National Research Council of Canada, Ottawa, Ontario.

NBCC. (1960). "National Building Code of Canada 1960." National Research Council of Canada, Ottawa, Ontario.
NBCC. (1965a). "National Building Code of Canada 1965." National Research Council of Canada, Ottawa, Ontario.
NBCC. (1965b). "Supplement No. 3 to the National Building Code of Canada 1965 - Structural information for building design in Canada." National Research Council of Canada, Ottawa, Ontario.
NBCC. (1970a). "National Building Code of Canada 1970." National Research Council of Canada, Ottawa, Ontario.
NBCC. (1970b). "Supplement No. 4 to the National Building Code of Canada 1970 - Canadian structural design manual." National Research Council of Canada, Ottawa, Ontario.
NBCC. (1975a). "National Building Code of Canada 1975." National Research Council of Canada, Ottawa, Ontario.
NBCC. (1975b). "Supplement No. 4 to the National Building Code of Canada - Commentaries on Part 4 of the National Building Code of Canada 1975." National Research Council of Canada, Ottawa, Ontario.
NBCC. (1977). "National Building Code of Canada 1977." National Research Council of Canada, Ottawa, Ontario.
NBCC. (1980a). "National Building Code of Canada 1980." National Research Council of Canada, Ottawa, Ontario.
NBCC. (1980b). "Supplement to the National Building Code of Canada 1980." National Research Council of Canada, Ottawa, Ontario.
NBCC. (1985a). "National Building Code of Canada 1985." National Research Council of Canada, Ottawa, Ontario.
NBCC. (1985b). "Supplement to the National Building Code of Canada 1985." National Research Council of Canada, Ottawa, Ontario.
NBCC. (1990a). "National Building Code of Canada 1990." National Research Council of Canada, Ottawa, Ontario.
NBCC. (1990b). "Supplement to the National Building Code of Canada 1990." National Research Council of Canada, Ottawa, Ontario.
NBCC. (1995a). "National Building Code of Canada 1995." National Research Council of Canada, Ottawa, Ontario.
NBCC. (1995b). "User's Guide - NBC 1995 Structural Commentaries (Part 4)." National Research Council of Canada, Ottawa, Ontario.
NBCC. (2005a). "National Building Code of Canada 2005." National Research Council of Canada, Ottawa, Ontario.
NBCC. (2005b). "User's Guide - NBC 2005 Structural Commentaries (Part 4 of Division B)." National Research Council of Canada, Ottawa, Ontario.
Oppenheim, A. V., and Schafer, R. W. (1975). *Digital signal processing*, Prentice-Hall, Englewood Cliffs, New Jersey.
Pan, T.-C., You, X., and Brownjohn, J. M. W. (2006). "Effects of infill walls and floor diaphragms on the dynamic characteristics of a narrow-rectangle building." *Earthquake Engineering and Structural Dynamics*, 35, 637-651.
Parloo, E., Guillaume, P., and Cauberghe, B. (2003). "Maximum likelihood identification of non-stationary operational data." *Journal of Sound and Vibration*, 268(5), 971-991.

Proakis, J. G., and Manolakis, D. G. (1988). *Introduction to digital signal processing*, Macmillan Publishing Company, New York, NY.
Proulx, J., Paultre, P., Rheault, J., and Robert, Y. (2001). "An experimental investigation of water level effects on the dynamic behaviour of a large arch dam." *Earthquake Engineering and Structural Dynamics*, 30, 1147-1166.
Roberts, R. A., and Mullis, C. T. (1987). *Digital signal processing*, Addison-Wesley Publishing Company, Reading, Massachussets.
Saatcioglu, M., and Humar, J. (2003). "Dynamic analysis of buildings for earthquake-resistant design." *Canadian Journal of Civil Engineering*, 30, 338-359.
Schiff, A. J. (1972). "Identification of large structures using data from ambient and low level excitations." in System Identification of Vibrating Structures, W. D. Pilkey and R. Cohen, eds., ASME, New York, NY.
Schott, J. R. (2005). *Matrix Analysis for Statistics*, Wiley & Sons, Hoboken, NJ.
Tremblay, R. (2005). "Fundamental periods of vibration of braced steel frames for seismic design." *Earthquake Spectra*, 21(3), 833-860.
Trifunac, M. D. (1972). "Comparisons between ambient and forced vibration experiments " *Earthquake Engineering and Structural Dynamics*, 1, 133-150.
Trifunac, M. D., Ivanovic, S. S., and Todorovska, M. I. (2001a). "Apparent periods of a building. I: Fourier analysis." *Journal of Structural Engineering*, 127(5), 517-526.
Trifunac, M. D., Ivanovic, S. S., and Todorovska, M. I. (2001b). "Apparent periods of a building. II: Time-frequency analysis." *Journal of Structural Engineering*, 127(5), 527-537.
Udwadia, F. E., and Trifunac, M. D. (1974). "Time and amplitude dependent response of structures." *Earthquake Engineering and Structural Dynamics*, 2, 359-378.
Van Overschee, P., and De Moor, B. (1993). "Subspace algorithms for the stochastic identification problem." *Automatica*, 29(3), 649-660.
Weber, B., Paultre, P., and Proulx, J. (2007). "Structural damage detection using nonlinear parameter identification with Tikhonov regularization." *Structural Control and Health Monitoring*, 14, 406-427.
Yang, J. N., Lei, Y., Pan, S., and Huang, N. (2003). "System identification of linear structures based on Hilbert-Huang spectral analysis. Part 1: Normal modes." *Earthquake Engineering and Structural Dynamics*, 32, 1443-1467.
Yuen, K.-V., and Katafygiotis, L. S. (2005). "Model updating using noisy response measurements without knowledge of the input spectrum." *Earthquake Engineering and Structural Dynamics*, 34, 167-187.